

Chapter 3

Synthesis and Characterization of Sr_2CeO_4 : with various routes and positive features of sol-gel technique

3.1 Introduction

The phosphor research has taken a great shape and the current trends in the research and development are to make the use of newer and older methods to make the research viable today. The need of the hour is to revolutionize the synthesis technique and modify it according to the needs of the day. Solid state has been and is still being used as a very common technique to develop phosphor either at laboratory level or commercial level, but there is a remarkable shift in the paradigm with the advent of nanotechnology which is now driving the industry forward towards an unknown and unprecedented phase, where the small is gaining and the big is losing literally. The concentration of the research at minute level are throwing challenges which were neither seen nor heard before, but still the exploration of 'Small' is definitely the 'thing' which one is looking at. The 'Small' in the phosphor is still in its early days though a remarkable understanding and research on the same is going on. When Bhargava et al.[1] published their paper that even the 'Small' was more efficient than the bulk and the size dependence with the efficiency had an optimistic trend, it was noticed and a way was set for the research to go directional.

Nanometer-sized phosphor powders exhibit spectroscopic properties that are different from their micrometer-sized counterparts. Generally, the observed luminescence in nanocrystalline materials has been explained using two arguments:

- (1) luminescence is dominated by quantum confinement effects and
- (2) luminescence is dominated by defect interactions and chemical species [2].

Nobel Laureate Late Sir Richard Feynman's famous lines "There is plenty of room at the bottom", yes there is plenty and there was plenty but we have to use and apply our brain to get the optimum out of that room.

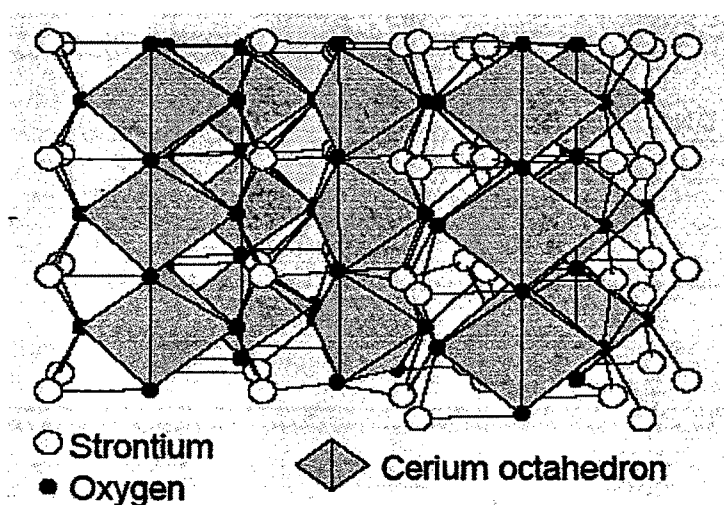
For the last one and half decade the nanotechnology, with size limitation of less than 100nm, has been moving at a pace and gaining momentum, research in this field is becoming more and more active [3, 4]. In this regard the phosphor research has also awakened to the challenge and new and better materials with the size limitations are being pursued rigorously. A number of publications have appeared on the same and the effect on the size with the effect on the optical

property has been a topic of great interest today. The goal of this research effort was to develop a comprehensive understanding of the factors that affect the luminescence behavior and study the optical properties of synthesized (using sol-gel method) nanocrystal phosphors with crystallite sizes less than 100nm. Up till now the commercial phosphors are synthesized using solid state reaction which requires the raw materials to be ground using an high speed grinders/ball mills and fired at 1200-1600°C or more depending on the synthesis temperature for many hours with two or more intermediate grindings. Of late, much emphasis has been given to improve upon the synthesis technique so as to improve the optical properties of the phosphor without losing on the efficiency.

3.2 Structure and Fundamentals of Sr_2CeO_4

3.2.1 Fundamental knowledge of structure and chemistry of Sr_2CeO_4 , characteristics, factors that impart luminescence

The information of the structure of phosphor would give an insight to the mechanism and the chemistry. Structural parameters influence in determination of luminescence characteristics of the phosphor. Knowing the structure leads to gaining the knowledge about the type of doping one has to do to increase the efficiency, output and thus the luminescent character of the phosphor. Danielson et al [5] discovered a new luminescent material by combinatorial material synthesis having an octahedral structure as shown in structure-1 below.



Structure-1 Sr_2CeO_4 -Analytical Chemistry Structure.

3.2.2 Influence of the host

The influence of different host lattices on a given luminescent centre results in a different optical properties. For the field of material science this is of primary importance if we could understand how the luminescence properties of an optical center depend on the host lattice, it would be easy to predict all the luminescent materials. There are few factors responsible for the different spectral properties of given ion in different host lattices. One of them is covalency, increasing covalency the interaction between the electrons is reduced, since they spread out over wider orbitals. Higher covalency effects the electronegativity difference between the constituting ions which becomes less and thus the CTT (charge transfer transitions) between these shift to lower energy. Another factor responsible for the influence of the host lattice on the optical properties of a given ion is the crystal field. Crystal field is also one of the factor responsible for the splitting of certain optical transitions [6].

3.2.3 Different synthesis techniques

The aim of the thesis revolves around the synthesis and characteristics of Sr_2CeO_4 , so different synthesis conditions are applied for the preparation of the phosphor. Up till now most of the phosphor material produced was by solid state reaction whose disadvantages would be discussed as we go through the length of this chapter. With the ever increasing demand for improvement, phosphors synthesis with many chemical processes is being tried. Danielson and coworkers [5] had prepared a blue phosphor (Sr_2CeO_4) by combinatorial material synthesis, after this a number of papers have been published on the preparation of this phosphor by other synthesis techniques like solid state reaction [7], chemical coprecipitation process [8], microwave calcination technique [9], ultrasonic spray pyrolysis technique [10], pulsed-laser deposition procedure [9, 11], Pechini's method [12], citrate-gel method [13], combustion method [14], microwave-accelerated hydrothermal technique [15], polymer synthesis [16], Wet chemical method [17], Emulsion liquid membrane system [18, 19], Sol-Gel by single alkoxide precursor [20], laser ablation [21], microemulsion method [22], carbonate precursor [23] have been tried to synthesize the same material. Some of

the above techniques require higher firing temperature i.e. above 1200°C [8, 11], whereas all the other synthesis methods mentioned above state that the compound formation was done only at 900°C-1100°C [5, 7, 9, 10, 12-18]. Some of these techniques of low firing temperature require firing for longer durations at elevated temperatures, while some of them require very expensive and not easily available starting materials [19]. The very high cost, difficulty in controlling the experimental process and toxicity of the alkoxide precursors used in this type of sol-gel process are some of the disadvantages of single alkoxide sol-gel preparation [24]. Moreover the sophisticated equipments used for many of the above type of synthesis are not easily available in every laboratory. The materials prepared by these techniques show less homogeneity, and large crystal size. Taking into consideration all these factors, we prepared Sr₂CeO₄ by sol-gel technique to achieve good homogeneity and better luminescent properties. This synthesis route is very easy and does not require expensive chemicals as well as sophisticated equipments [25]. The surface area of the powders produced from the sol-gel is very high as well as the cross contamination is low. Our interest is not only to develop this material by sol-gel but also to try and achieve a uniform particle size within the nanometer range which present new and interesting observations to light. It has been an endeavor of scientists and researchers across the globe to study sol-gel due to its easy approach for synthesis.

In this chapter the detailed description of synthesis of the phosphor by various techniques with their drawbacks are discussed. The Sr₂CeO₄ phosphor is prepared by three techniques, as:

- A. Solid State Reaction Technique.
- B. Sol-Gel Technique.
- C. Combustion Synthesis Technique.

3.3 Sol-gel Technique and its positives with respect to the Sr_2CeO_4 phosphor

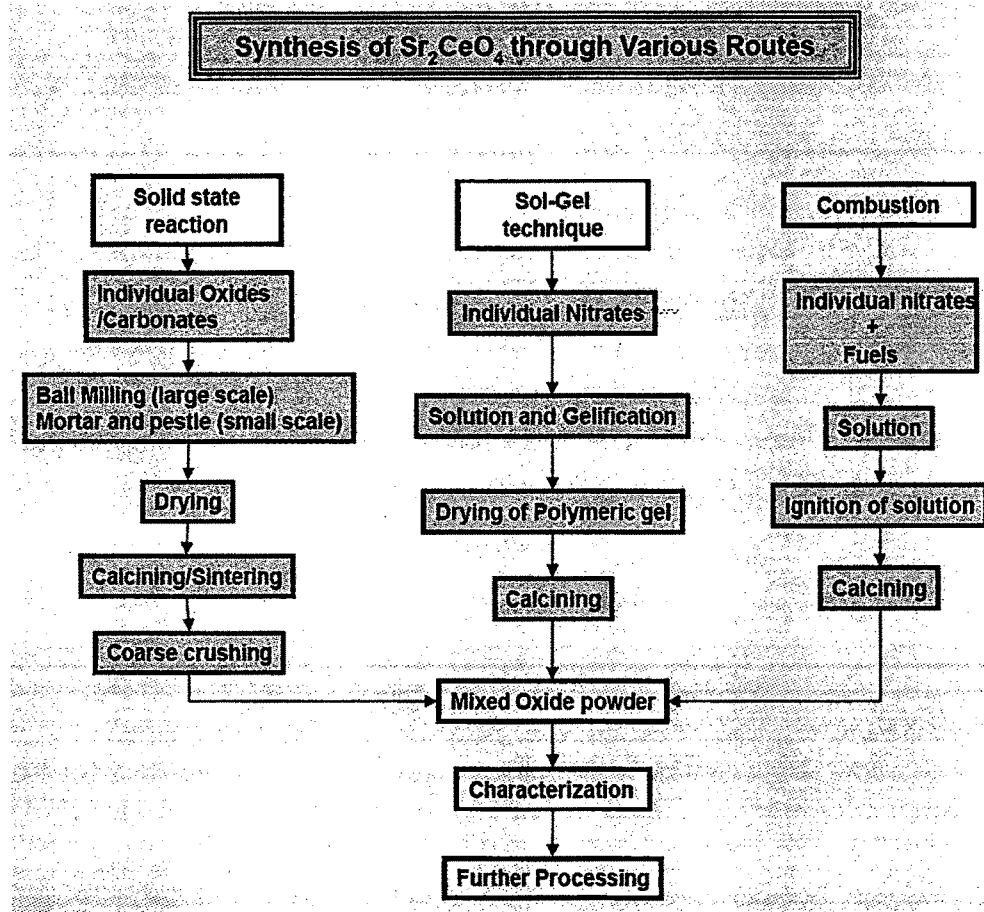


Chart-1 Represents a schematic diagram of all the synthesis technique applied to make the phosphor.

3.3 A. Solid State Reaction

Almost all rare earth activated phosphors are synthesized by solid state diffusion reaction between the raw materials at high temperature. Although the basics of the industrial scale phosphor synthesis were well established decade ago, the process optimization is still continuing because of the importance for phosphor efficiency required for different applications, the production cost and hence market share. The synthesis of a phosphor with reproducible efficiency and

chromaticity requires careful control on the purity, stoichiometry and particle size of the starting raw materials. Chart-1 gives the general concept of phosphor synthesis process. First the high purity materials of the host crystal, activators, and the fluxes are blended, mixed and then fired in a container. As the product obtained by firing is more or less sintered, it is crushed, milled and then sorted to remove coarse and excessively crushed particles. In some cases the product undergoes surface treatment. This is the easiest and most popular synthesis technique used till date. The commercial phosphors are still pursued with the same technique. Preparation of single phase compound is difficult by the conventional solid state method. Hence, doping a low concentration (of the order of 1–3%) of activator has always been delicate. Thus, the limitations of conventional solid state method are:-

1. Inhomogeneity of the final product.
2. Formation of large particles with low surface area and hence, mechanical particle size reduction (ball milling) required, which introduces impurity and defects.
3. Presence of defects, which are harmful to luminescence emission.
4. Milling and grinding the phosphor results in a substantial decrease in luminescence efficiency, however, this is normally attributed to an increase in non-radiative recombination via surface defect states as particle size decreases, i.e., the formation of a surface dead layer [26, 27, 28].

The problem of inhomogeneity could be mitigated by the use of non-conventional methods (wet-chemical) [28].

The starting materials taken for solid state reactions were SrCO_3 , CeO_2 purchased from S.D. fine chemicals (Boisar). The stoichiometric ratio of Sr:Ce was taken as 2:1. The samples were first grinded using agate mortar and pestle and then kept in a furnace. The temperature of the furnace was gradually increased to 1200°C from the room temperature. The heating rate of the furnace was fixed at $6.67^\circ\text{C}/\text{minute}$. The samples were kept in the furnace at 1200°C for 10 to 30 hours with two or three intermediate grindings. After the heating was done, the sample was allowed to cool by switching it off. The samples were again grinded using agate mortar and pestle. The resulting powder was white in colour.

3.3 B. Sol-Gel Technique

Materials chemistry is a field of high priority internationally, both in terms of fundamental and applied science. Research contributions to the advancement of this field come from a wide range of scientists who develop the synthetic processes, design the blends to produce the desired properties, perform the fundamental characterizations, and employ them in a wide range of applications. One of the synthetic processes of great interest at present is sol-gel chemistry. The sol-gel process, which was discovered over 150 years ago, was originally a method for the production of ceramic materials. However, it was not until the 1960's that sol-gel research emerged as a major field of study [29]. It is a very simple and economical method for making high-quality luminescent materials. The solution-based sol-gel method is one of the most important techniques for the synthesis of ceramics, because it possesses a number of advantages over conventional techniques, such as low-temperature processing, easy coating of large surfaces, and possible formation of porous films and homogeneous multicomponent oxide films [29]. The flow chart of the sol-gel technique is also made in chart-1. For most of the synthesis the sol-gel precursors used are metal alkoxides and/or organometallic compounds, which suffer from the disadvantages of high cost, toxicity, and difficulty in controlling the experimental processes. An alternative approach to this is Pechini-type sol-gel process, which mainly employs inorganic salts as precursors, citric acid as the chelate ligand, and ethylene glycol (EG) as the cross-linking agent [24, 30-32]. Efforts have been made to develop various kinds of luminescent film via a sol-gel method in the past decade. There are excellent reviews and papers available that have commented on the many positives the sol-gel offers, discussed at length in the introduction, over various synthesis techniques [34-39].

The concentration of the work is on the synthesis by sol-gel, much of the work has been to develop this synthesis technique for our materials. The starting materials taken were $\text{Sr}(\text{NO}_3)_2$, $\text{Ce}(\text{NO}_3)_3 \cdot 6\text{H}_2\text{O}$, Citric Acid, Ethylene Glycol and Liquid ammonia (NH_3) purchased from S.D. fine chemicals (Boisar, Mumbai, India). The stoichiometric ratio of Sr:Ce were taken in 2:1. The nitrates were first dissolved in around 20ml of double distilled water and kept for stirring on a magnetic plate at room temperature until it becomes transparent in color and all the salt have mixed. Gradually the temperature of the plate was increased to 40-

50°C. After a certain time of continuous stirring, citric acid was added to the transparent solution. The pH of the resulting solution was maintained 6-7 by adding droplets of ammonia. The temperature of the solution was raised to 60-80°C. The solution at this stage becomes milky in colour due to the precipitation taking place in the solution due to citric acid acting as a chelating agent. After few hours of stirring Ethylene glycol was added to the solution and stirring was maintained. The solution now changes its colour and becomes yellow, becoming more viscous and the formation of gel takes place. The starting materials used are nitrates in aqueous media, which form stable gels through gelation with citric acid, followed by cross-linking after polycondensation of ethylene glycol at increased temperature. The synthesis of Sr_2CeO_4 by sol-gel has been shown in chart-2. This mechanism ensures that the gel formation takes place. The gel is then kept in an oven at 110°C for 4 hours to remove water content if any and for drying. The dried gel was then made into 4 parts. Each part was given a different heat treatment.

Part- 1 A – Kept for heating at 400°C for 2 hrs.

Part- 2 B – Kept for heating at 800°C for 4 hrs.

Part- 3 C – Kept for heating at 1000°C for 4 hrs.

Part- 4 D – Kept for heating at 1200°C for 2 hrs.

Synthesis of Sr₂CeO₄ through Sol-Gel

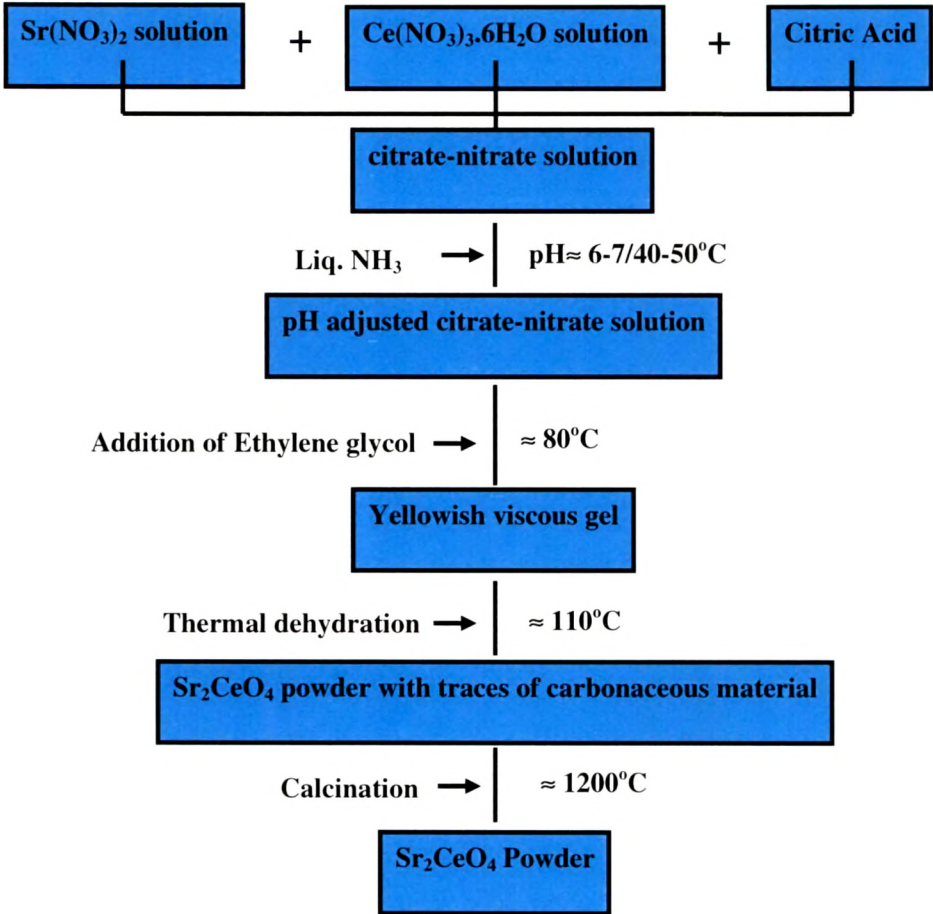


Chart-2 Synthesis of Sr₂CeO₄ through Sol-gel technique.

3.3 C. Combustion Synthesis

To overcome the limitations of the solid state reaction process, new and older synthesis techniques have been applied to synthesize phosphors. In this regard the sol-gel and combustion synthesis techniques have been equally explored. The successful synthesis of nanocrystalline material can be achieved by a number of processes, including sol-gel techniques or gas-phase condensation and or combustion technique [26, 27, 40]. These are becoming popular for making phosphors with size limitations and better optical properties. The positive features of the sol-gel techniques would be elaborated by us, but for comparison we also have synthesized some samples by the combustion technique also, which off late, due to its easy synthesizing conditions is becoming a favourite. Combustion technique [41, 42] is another wet-chemical method which does not require further calcinations and repeated heating. This method was accidentally discovered in 1988 in Prof. Patil's lab at Indian Institute of science, Bangalore, India. A number of publications from the group at IISc [28, 41-51] and also world over have been published using this technique [40, 52-58]. Phosphor synthesis by these have resulted in reduced particle size $> 100\text{nm}$ [40, 54-58] so it was of interest to us to check its applicability in our case too. Combustion process results in an exothermic reaction and occurs with the evolution of heat and light which leads to formation and crystallization of phosphor materials. For any combustion reaction to occur, fuel and oxidizer are required. For the combustion synthesis of oxides, metal nitrates are used as oxidizer, and fuels employed are hydrazine based compounds or urea or glycine. Though a number of fuels so far employed for the reactions are glycine, urea, oxalyldihydrazide, carbohydrazide, etc but in this study we limit ourselves to urea and citric acid as most of the others are carcinogenic, especially hydrazine derivatives [40]. Moreover the used two are inexpensive, readily available and can be used for preparation of large variety of oxides. Stoichiometric compositions of metal nitrates and fuels are calculated based upon propellant chemistry. Thus, heat of combustion is maximum for O/F ratio 1 [41]. Based on the concepts used in propellant chemistry [41], the elements C, H, V, B or any other metal are considered as reducing elements with valencies +4, +1, +5, +3 (or valency of the metal ion in that compound), respectively and oxygen is an oxidizer having the valency of -2. The valency of

nitrogen is taken as zero because of its conversion to molecular nitrogen during combustion.

When properly controlled, high temperatures are generated by the exothermic redox reactions between the decomposition of the salts and the fuel. As a result of fast heating and cooling, there is little growth of crystals, which produces the nanoceramics. Few workers have studied the effect of different fuel to oxidizer ratio (F/O) [40, 53-55], they reported that the average particle size of their nanophosphor prepared by the combustion method was dependent on the ratio of organic fuel used in the combustion. These studies inspired us to check the suitability of the F/O ratio for our material. Along with the sol-gel technique for the preparation of nanocrystalline materials combustion was also tried. The starting materials taken in this were $\text{Sr}(\text{NO}_3)_2$, $\text{Ce}(\text{NO}_3)_3 \cdot 6\text{H}_2\text{O}$ and the fuel used were urea and citric acid (All the materials were purchased from S.D. fine chemicals). The stoichiometric ratio of Sr:Ce was kept at 2:1. The nitrates of both the salts were mixed with 10 ml of double distilled water and kept at for stirring on a magnetic stirrer for 2 hrs until the starting materials have mixed homogeneously. Then fuel citric acid/urea were added to the solution and stirred for 1 hour. The solution was then kept in the furnace which was already maintained at $500^\circ\text{C} \pm 10^\circ\text{C}$. The solution boils, foams and ignites to burn with flame to yield voluminous, foamy compound with the release of black fumes and the sample occupying whole volume of the container. The entire combustion process lasted for about 5 minutes. The combustion process is self-propagating i.e., once ignited it goes to completion without the supply of additional heat from an external source. The resulting powder was very soft and white in colour. This was again made in two parts. Part A kept was as used and Part B was further heated at 1200°C for 4 hrs. Flow chart for the synthesis is shown in chart-1.

In the case of Sr_2CeO_4 , as per the propellant chemistry [28, 52] following are the valencies of the elements calculated. The fuels used for the combustion synthesis are urea and citric acid. Valency of Strontium (Sr) is +2, Cerium has +3 valency and valency of $(\text{NO}_3)_2$ was calculated as (-12).

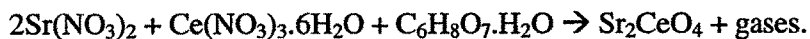
Therefore the equation for the synthesis of the Sr_2CeO_4 becomes (when urea is used as fuel):



The stoichiometric ratio for Sr_2CeO_4 , when urea is used as fuel is:

2:1:5.8333

The equation for the synthesis of the Sr_2CeO_4 becomes (when is **Citric Acid** is used as fuel):



The stoichiometric ratio for Sr_2CeO_4 , when **citric acid** is used as fuel is:

2:1:1.944

Compound	Stoichiometry
$\text{Sr}(\text{NO}_3)_2$	2
$\text{Ce}(\text{NO}_3)_3$	1
Urea, $\text{NH}_2 \cdot \text{CO} \cdot \text{NH}_2$	5.833
Citric Acid, $\text{C}_6\text{H}_8\text{O}_7 \cdot \text{H}_2\text{O}$	1.944

Table-1 Stoichiometry ratio for all the starting compounds.

Compound	Valency
$\text{Sr}(\text{NO}_3)_2$	-10
$\text{Ce}(\text{NO}_3)_3$	-15
Urea, $\text{NH}_2 \cdot \text{CO} \cdot \text{NH}_2$	+6
Citric Acid, $\text{C}_6\text{H}_8\text{O}_7 \cdot \text{H}_2\text{O}$	+18

Table-2 Oxidizing and reducing valencies of metal nitrates and fuels.

In the literature there are very few reports which mentions the effect of Fuel to metal (hereafter referred to as F/M) ratio on the size and the optical properties of the phosphor. As the variation of this changes the stoichiometric ratio which thus leads to a change in the adiabatic flame temperature with a direct effect on the size of the phosphor [54, 55]. Hence to observe the variation in the photoluminescence characteristics of the Sr_2CeO_4 phosphor we varied the F/M ratio by some proportion and the results are discussed as we go through the length of this chapter. In these experiments also, the samples were further heated at 1200°C for 3hrs, we have also compared the as synthesized Sr_2CeO_4 powders by combustion technique.

3.4 Characterization

3.4.1 X-ray Diffraction studies

Phase identification of the powders was carried out by the X-ray powder diffraction using RIGAKU D'MAX III Diffractometer having Cu K α radiation ($\lambda = 0.154\text{nm}$). The scan range was kept from 5 degrees to 80 degrees at the scan speed of 0.05 degree per second.

3.4.2 Scanning Electron microscopy (SEM)

The Scanning Electron Micrograph images (SEM) of the samples were taken using JEOL make JSM-5610 LV for studying the morphology of the compound, details in chapter two.

3.4.3 (a) Photoluminescence measurements

The photoluminescence (Emission and Excitation spectra) were recorded at room temperature using spectrofluorophotometer RF-5301 PC of SHIMADZU make, details in chapter two. The source used in this is a xenon lamp. The slit width for the emission and excitation was kept at 1.5nm for all the measurements. A filter was used to remove the second order peak of the excitation light in the PL measurements. The sensitivity of the instrument was set as high unless stated otherwise.

3.4.3 (b) Thermoluminescence measurements

The thermoluminescence glow curves were recorded with Nucleonix TL-setup, the details of which have been discussed in chapter two.

3.4.4 Commission Internationale de' Eclairage (CIE)

For the present study, the *Equidistant-Wavelength method* has been used to determine the coordinates on the colorimetric chromaticity diagram. The CIE coordinates for the samples have been calculated for CIE 1931, CIE 1960 and CIE 1976, details have been given in chapter two.

3.5 Result and Discussion

3.5.1 X-ray diffraction studies (Powder)

All the samples were then subjected to various characterizations. The X-ray diffraction of the samples for solid state reaction revealed that the samples formation was only possible at 1200°C.

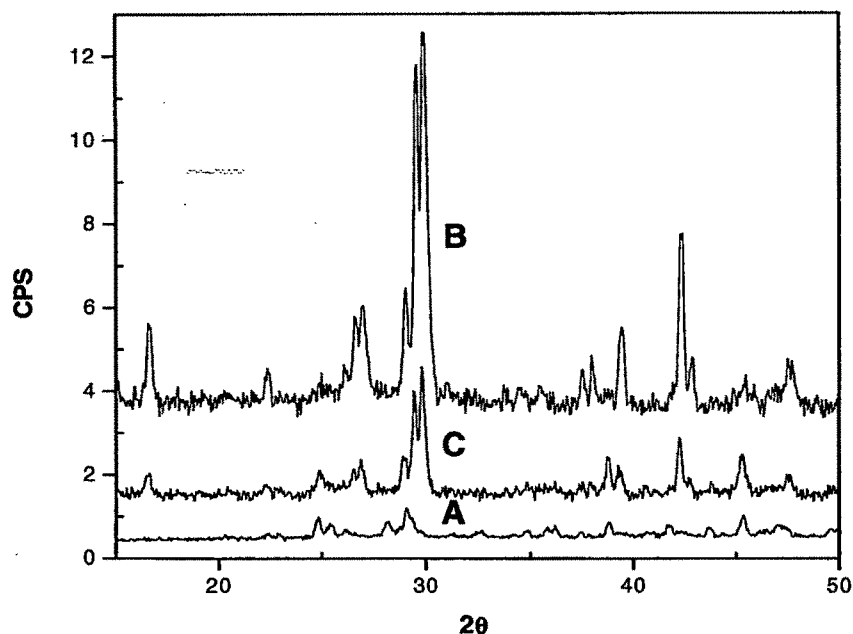
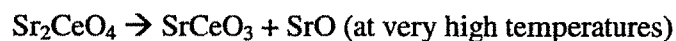
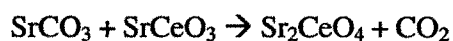
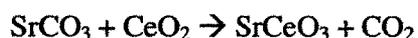


Figure-1 X-ray Diffraction patterns of the samples A, B and C.

The figure-1 shows the XRD pattern of the samples for solid state and sol-gel synthesized, the curves A, B and C stands for sample heated at 800, 1200 and 1200°C for sol-gel and solid state respectively. As reported earlier also that the phase formation of the compound is an important step to proceed to next step of spectroscopic study. The pure phase formation as reported in earlier studies was also at 1200°C for 20-48-60 hrs [5, 23, 59, 60]. Pure phase formation at lower temperature i.e. between 900-1100°C [12] have not been reported. Serra et al had also synthesized the phosphor by Pechini Sol-Gel but even they have clearly mentioned that the XRD pattern revealed the additional phases of CeO₂ when fired at 1100°C from 2-4 hrs and/or in the absence of pure oxygen flux. Y.Tang et al. [9] have mentioned that it was impossible to measure the temperature and

control the sample in the microwave cavity, the heat generated inside is unknown. An important observation by Chavan et al [61] was that the phase Sr_2CeO_4 was obtained only when the sample was heated at 1050°C for 60 hrs with three intermediate grindings [62]. It required 950°C for 5 hrs and then again 1100°C for 8 hrs in air by wet chemical method and 1100°C for 2 hrs and 1300°C for 24 hrs in dried air by solid state reaction [17, 63]. Xibin Yu et al reported in 2003 about the citrate-gel synthesis, they fired at various temperatures from 700°C to 1000°C for 2 hrs in muffle furnace in air; they elucidated the fact that this material was not pure with traces of Ce_4SrO_7 present in it [13]. Polymer sol-gel route was also tried to make the same and the temperature kept at 1100°C for 10 hrs in air [16]. In another reported work by Khollam et al by microwave – accelerated hydrothermal synthesis the material was fired at 1000°C for 5, 8, and 25 hrs respectively, they found that the pure phase was still not achievable with traces of SrCeO_3 still present [15]. Gomes et al [14] reported the same at 950°C for 4 hrs in air by combustion. Hirai et al [18, 19] reported that by using an emulsion liquid membrane system (thin film at 900°C for 2 hrs) followed by firing at 1000°C for 2 hrs in air, they found that the ratio of Sr/Ce was more than two if the Sr_2CeO_4 has to be formed i.e. the starting ratio should be un-stoichiometric. Xing et al used the micro-emulsion-heating method [22] taking oxalate as the starting materials fired at 1100°C for 4 hrs and the final product Sr_2CeO_4 was obtained but they dried the sample in an oven at 120°C for 36 hrs (duration is very long for the sample to be made). Kim et al [20] used single alkoxide precursors whose serious drawbacks we have already discussed. Perea et al [21] reported the same using laser ablation and then sintering in air for 1260°C for 3hrs. Shikao Shi et al [23] reported the same by carbonate precursor and fired at 1200°C for 3hrs but still traces of SrCeO_3 could be found. Kang et al [64] kept the sample inside a special ultrasonic spray pyrolysis apparatus and the heat was varied from 600 - 1100°C with a continuous flow of nitrogen, however single phase was not reported at this temperature, moreover the drawbacks of this method is the formation of the hollow particles. Hong et al [65] had prepared the same by spray pyrolysis at 800 to 1600°C and then post-treated at temperatures between 700 to 1200°C for 3 hrs in muffle furnace and even with such sophisticated setups and high degree of heat provided to the sample pure phase could not be achieved. He et al [66] have prepared the same by co-precipitation at

1000°C for 2hrs, but they have used extremely sophisticated equipments like ultrasonic stirrer, Teflon vessel and an steel autoclave. Almost all the methods and the technique discussed above have some drawbacks which allow us to explore the sol-gel and to put forward the positives with respect to Sr₂CeO₄. We have found out that the phase formation of the compound when synthesized by the sol-gel method at 1200°C is the most pure and matching with the literature [67]. When the temperature of firing was 800°C it is found that there are some more phases present in the compound as SrO, SrCeO₃ etc, we estimate that the impure or unreacted material present in the compound at 800°C will react at higher temperature to result in the pure phase of Sr₂CeO₄ according to the equation below and further heating of the sample will result in decomposition of the phase [9]:



The heat of formation of the compound and the dissociation of it is already been discussed in the work by Pankajavalli et al.[68] they also used combustion route to prepare the Sr₂CeO₄ and heated further at 1100°C for 12 hrs and still traces of SrCeO₃ were found in it. Still as the temperature is raised to 1000°C, the compound has not resulted in the pure phase as it is quite possible that the reaction of the initial and intermediate product at 1200°C will only facilitate the phase formation. Thus we can say that the pure phase formation is achieved at 1200°C. The crystal structure was found to be orthogonal [67] and not triclinic [69] as reported in most of the literature cited for the Sr₂CeO₄. The lattice parameters were also reported to be a = 6.118Å, b = 10.349Å and c = 3.597Å respectively.

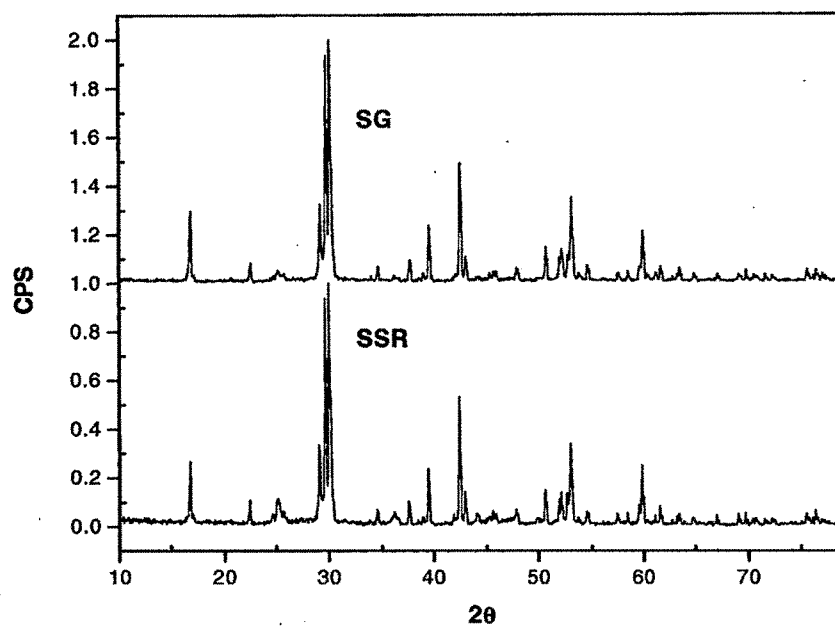


Figure-2 The X-ray diffraction pattern of the sol-gel and solid state synthesized sample at 1200°C.

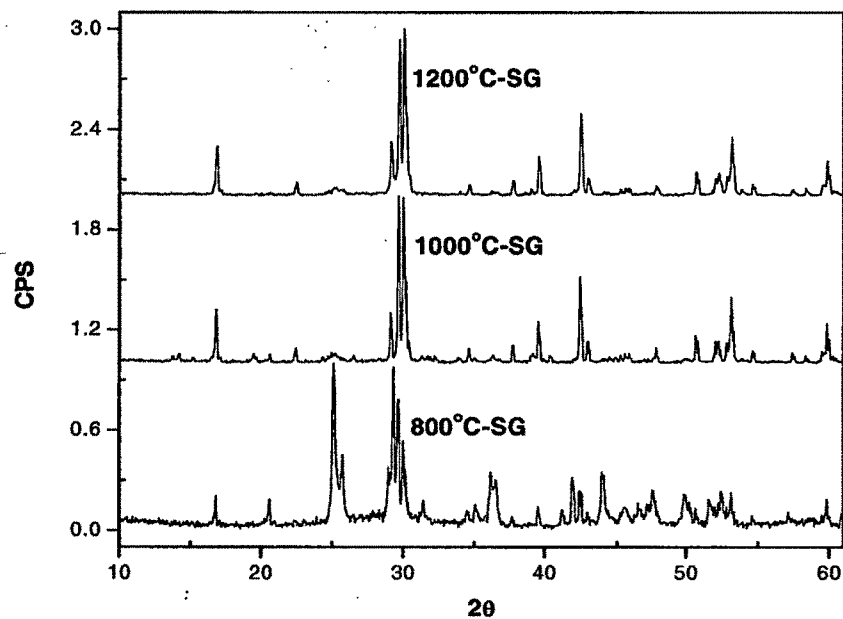


Figure-3 The X-ray diffraction pattern of the sol-gel synthesized sample at different temperatures.

Figure-2 is the sol-gel and solid state synthesized sample at 1200°C and it is observed that the sample forms only at 1200°C, and there is hardly any difference X-ray diffraction pattern and matches well with the literature. Figure-3 is the X-ray diffraction pattern of the sol-gel synthesized sample at 800°C, 1000°C and 1200°C respectively and it is observed that the pure phase is formed only at 1200°C and at lower temperatures there are traces of SrCeO₃, CeO₂ and Sr(NO₃)₂ present in the samples which gets removed at the higher temperature of 1200°C. This confirms our presumption of the pure phase formation at 1200°C with sol-gel. The data of our sample was matching with those of Mastromonaco et al [69], but again checking the results we found that the very weak reflections in the X-ray diffraction pattern were neglected by us. This was also put forward by Danielson et al.[5], in their paper.

The crystallite size determination was done by the Scherrer equation already discussed in chapter-2:

$$d = \frac{k \lambda}{\beta \cos \theta_B} \text{----- (1)}$$

where, d = thickness of the crystal (in angstroms),

k = constant (0.9),

λ = X-ray wavelength (0.1540nm for the present case),

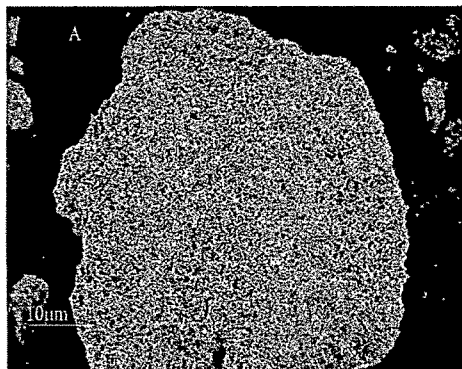
θ_B = Bragg angle,

β = Line Broadening (Full width Half-maximum in radians).

The average crystallite size comes out to be 45nm for the 1200°C sol-gel prepared and it comes out to be 155nm for the one synthesized by solid state reaction. The formation of nanocrystallite size from the sol-gel is a desired property. The effect of the size on the optical property of the Sr₂CeO₄ will be of great interest as we go through the length of this thesis. Till date there are very few reports that have mentioned the size of the Sr₂CeO₄ in nanometer range with respect to X-ray diffraction studies. Yu et al [13] reported the size to be 60nm from the X-ray diffraction pattern. Xing et al [22] reported the orthorhombic structure with size as 60nm for 850°C for 4hrs, 620nm for 1000°C for 4hrs and 690nm for 1100°C for 4hrs. The estimated data from the XRD by He et al [66] have been reported to be in the range of 60.2-79.6nm.

3.5.2 Scanning Electron micrograph

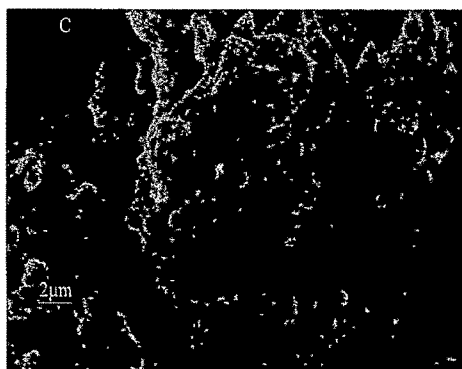
The SEM micrographs have been taken for the Sr_2CeO_4 prepared by different synthesis technique and at different temperatures. The SEM gives an insight into the morphology of the sample and also information regarding the shape and size of the particles.



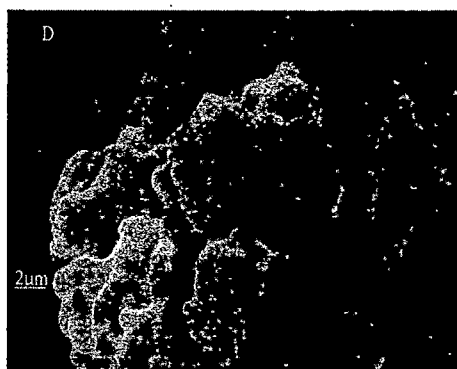
A. Solid state prepared at 1200°C.



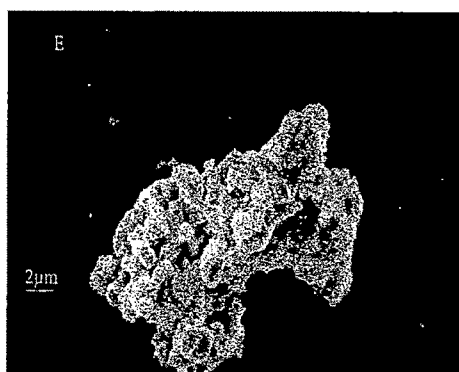
B. Solid state prepared at 1200°C.



C. Sol-Gel synthesized at 400°C.



D. Sol-Gel synthesized at 800°C.



E. Sol-Gel synthesized at 1200°C.

Scanning Electron Micrograph of the solid state and sol-gel prepared sample.

There are few reports which have commented on the size with respect to the SEM and TEM and these will be discussed as we go through the length of this chapter. Chen et al [16] reported that the SEM of their particle has the smallest particles less than 1 μ m with 200nm in diameter and 800nm in length with crotch like morphology. Kholam et al [15] reported that the SEM revealed spherical shape with \sim 0.5 μ m at 1000 $^{\circ}$ C/25hrs. Gomes et al [14] reported spheroidal particle with diameter between 250-550nm and by solid state reaction was more than 5 μ m in size. Hirai et al [18] reported the size to be in submicrometer ($>$ 100nm) but with the oxalate they found [19] of the size of \sim 60nm by SEM. Xing et al [22] reported that the SEM showed spherical shape under 100nm by their synthesis route and shuttle like shape for solid state reaction method. They also reported the change in the shape as the heating temperature was changed. Perea et al [21] reported by HRTEM, the grains size be 20-30nm diameter (building blocks) to form the film. With SEM, Kang et al [64] reported the mean size of the as prepared particle to be between 0.19 to 1.52 μ m but the main disadvantage of spray pyrolysis is the formation of hollow particles [65]. From TEM data He et al [66] have reported that the crystallite display rod-like monomorphology with the length of 50-150nm and width of about 80nm.

The Scanning Electron Microscopy studies have been done on the particles prepared by both the solid state as well as Sol-gel technique. All the SEM micrographs have been presented in the micrographs above. From the SEM micrographs one can see that the morphology of the samples prepared by the sol-gel is better. The shape and the size of the sol-gel prepared are round and they appear to be less agglomerated when compared with the solid state one. The solid state synthesized sample have been sintered and appear heavily agglomerated, the morphology is not uniform and they are tightly aggregated to one another to form large secondary particles. They also do not have narrow size distribution and appear very hard. The sol-gel synthesized samples are spheroidal in shape and even at high temperature of annealing they appear less agglomerated. The size of the sol-gel synthesized is very small compared to solid state and they appear very soft w.r.t solid state ones. This elaborates another positive of the sol-gel synthesis technique. As the firing temperature in the case of sol-gel synthesized sample was increased from 400 $^{\circ}$ C to 1200 $^{\circ}$ C the sample agglomerated a bit and as the temperature increased the shape and the size of the particles became spherical in

shape. The spherical morphology has a positive effect on the optical property, as the scattering of the light is less and hence it directly influences the luminescence intensity and will be discussed in the photoluminescence section. The sample synthesized by solid state reaction are very irregular in shape and are agglomerated as can be seen from the micrograph which is a very serious drawback concerning the solid state reaction. The better optical properties of the sample would give more insight to this fact.

3.5.3 Photoluminescence characteristics

3.5.3 (a) Luminescence from sol-gel and solid state synthesis technique

Photoluminescence is an important and powerful tool in analysis of surfaces and interfaces. The spontaneous emission of light from a material under optical excitation provide an insight to a variety of material parameters, it is a selective and very sensitive probe of discrete electronic states. Variation of the PL intensity with external parameters as temperature, voltage etc, can be used to characterize further underlying electronic states and bands. More information on this can be had from a recent review by Timothy Gfroerer [70]. In the present study all the Photoluminescence (PL) Characterization of all the samples were done at room temperature. The excitation and emission slit width was kept at 1.5nm in all the case with high sensitivity unless specified for different measurements. The Emission spectra of the phosphor synthesized at different temperatures was taken.

The Emission Spectra of the sample A, B & C at 254nm excitation

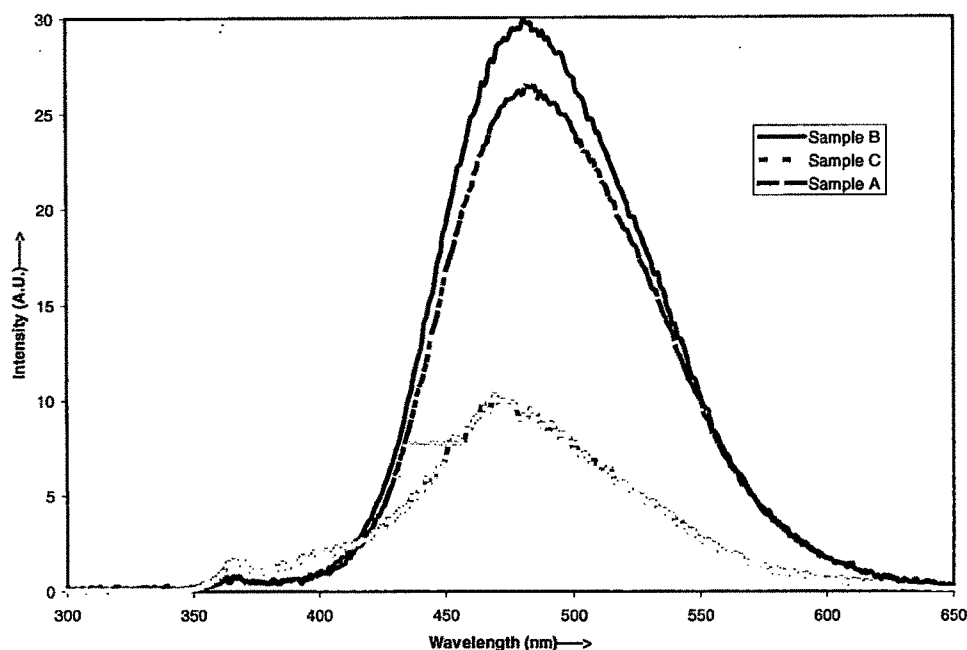


Figure-4 The photoluminescence emission spectra of the Sr₂CeO₄ sol-gel and solid state technique synthesized sample excited at 254nm wavelength.

The figure-4 is the emission spectra of the sample marked as A, B, C i.e. the sample synthesized with sol-gel technique at 800°C, 1200°C and by the solid state reaction at 1200°C respectively. As the temperature of firing was increased in the case of sol-gel prepared sample it was found that the photoluminescence intensity also increased, the same also observed in the X-ray diffraction pattern too. This can be attributed to the fact that as the temperature was increased from 800 to 1200°C the formation of pure phase occurred, the observed luminescence from the phosphor at 800°C was due to the fact that some amount of luminescent phase Sr₂CeO₄ was present at such a low temperature too and that has contributed to the PL spectra, as the other phases are non luminescent one can say that the Sr₂CeO₄ phase had appeared at less than 800°C. Another conclusion that can be drawn from this is that the crystallinity also increases as the temperature of firing is increased. The appearance of the broad band at ~472nm is attributed to the Ce⁴⁺→O²⁻ charge transfer transition. The appearance of charge transfer transition from Cerium is the first of its kind reported [5]. This is the kind of luminescence which is opposite to that of the phenomenon known as charge transfer absorption.

Though there is slight variation in the position of the appearance of the band which varies from 467nm (sample A) to 485nm (sample C) in the other. The reason still remains the same i.e. the charge transfer band. There is a considerable amount of difference in the intensity of the three samples with highest being for the sol-gel (B) one followed by the one by solid state (C). There is also a slight blue shift in the emission spectra of the sol-gel (A) curve as the particle size would be small at that temperature so it shows a slight difference. Though it was reported earlier that this may be due to the different synthesis techniques, but this does not appear so, as the shift is corresponds with both the sol-gel and solid state, the appreciable shift in the corresponding spectra may be a nanoeffect (the crystallite size of the sample A being the smallest). The setback that appears is that the sample A is not a pure phase of Sr_2CeO_4 and its intensity also very weak compared to the other two.

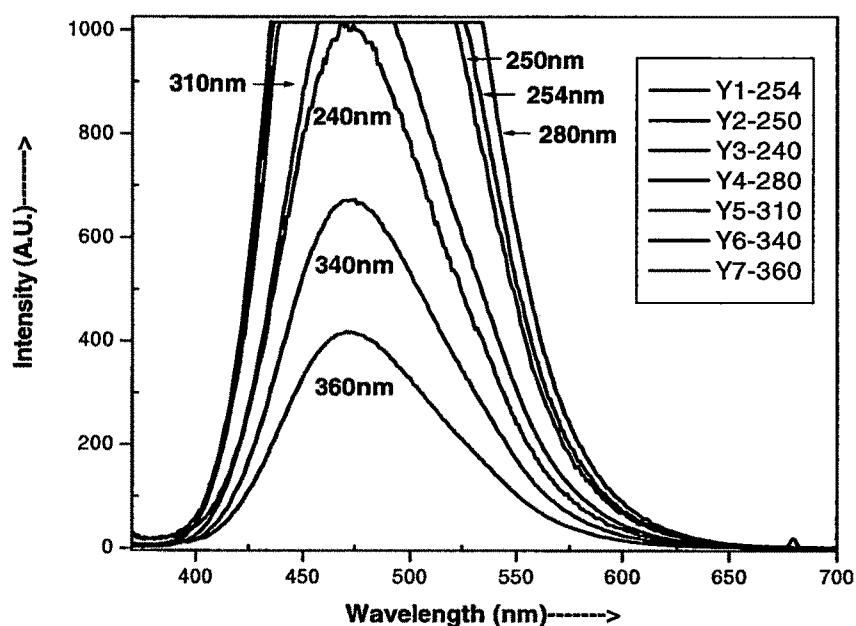


Figure-5 The photoluminescence emission spectra of the sol-gel synthesized sample at different excitation wavelengths.

The Sr_2CeO_4 sample prepared by sol-gel method was excited with different wavelengths from 240nm to 360nm for the 1200°C prepared sample, the interesting result that we can observe from the figure-5 is that the peak position

does not change much with the wavelength. Another interesting feature of these emission curves is that when the excitation wavelength was kept at 254nm the peak was very broad and it was of the highest intensity (out of range), also similar feature (out of range) was observed at 250nm, 280nm, 310nm with the next maxima at 280nm. The shape of the emission curve was same at all the wavelengths. This phosphor can thus be excited from a very large range of excitation (240nm to 340nm). Such type of broad excitation can be useful for many applications. Correlation of these with the excitation curves can lead to useful information on the nature and the origin of the luminescence. Annealing for longer duration increases the intensity, which may be due to the removal of oxygen vacancy related defect centers as also reported by Pieterse et al [59] and Nag et al [17]. We observe from the graph that despite the change in the excitation wavelength there is hardly any shift in the emission peak and/or there is almost no change in the shape of the curves, the variation is only in the intensity of the peaks which increases with maxima at 254nm and is appreciable at 280nm. The broad band of the emission starts from around 370nm peaks at 475nm (2.61eV) and ends at 570nm. This fact also elucidates our earlier conclusion that the sample kept for further heating had good intensity due to pure phase formation as described in the earlier sections.

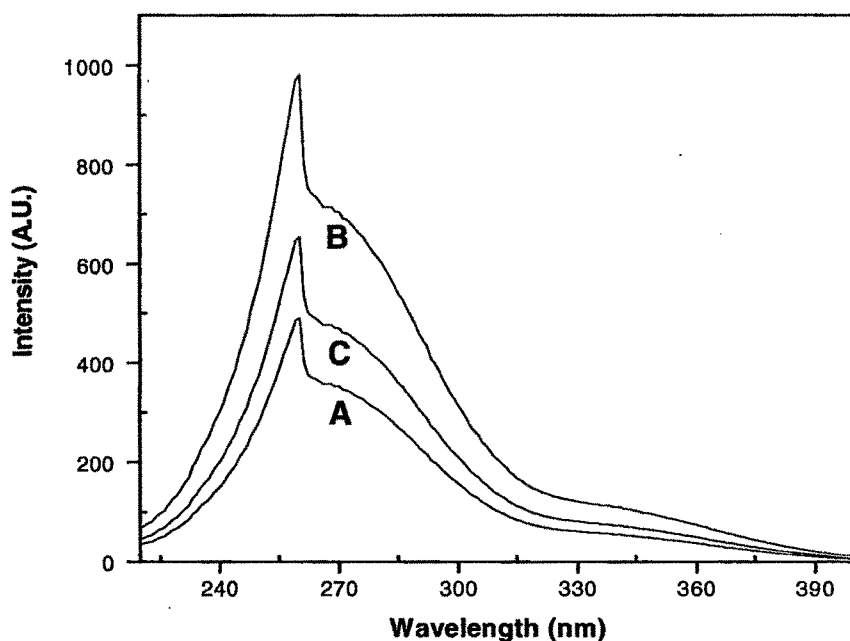


Figure-6 The photoluminescence excitation spectra of the Sr_2CeO_4 sol-gel and solid state technique synthesized sample monitored with 472nm wavelength.

The figure-6 is the photoluminescence excitation spectra of the sol-gel and solid state synthesized sample when monitored with. The sample was fired at 800C for 4hr (curve A) while the other one was fired at 1200C for 2hr (curve B), the other is the solid state synthesized sample heated at 1200C for 20hrs (curve C). The excitation peak was mainly observed at 254nm along with a small hump around 270nm (figure-6). This is mainly due to the charge transfer of the $\text{Ce}^{4+}-\text{O}^{2-}$ ligand as described by Danielson et al [5]. The two excitation peaks may be assigned to the two kinds of Ce^{4+} ions present in Sr_2CeO_4 . There are two different $\text{Ce}^{4+}-\text{O}^{2-}$ bond lengths in the lattice, thus two excitation peaks are attributed to the two different charge transfer transitions [5]. The hump around 270 nm evident from the excitation curve may be attributed to the above-defined mechanism. The thing to be noted here is that the intensity for the spectra of sample A is very less when compared with that of samples B and C. The intensity of sample B is the highest among all showing one of the advantages of this synthesis method.

3.5.3 (b) Photoluminescence emission and excitation spectra of combustion synthesized phosphors

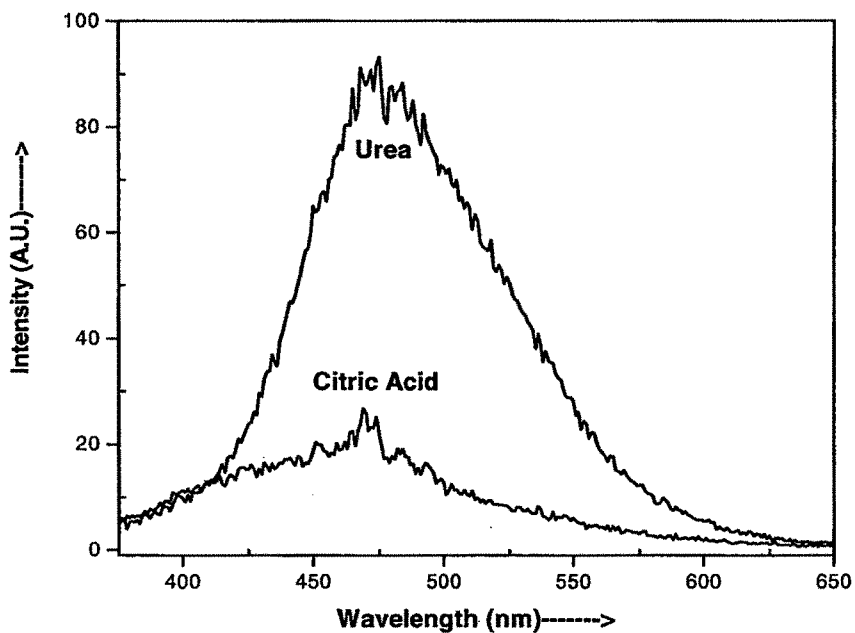


Figure-7 The photoluminescence emission spectra of the combustion synthesized sample with different fuels at 254nm excitation wavelength.

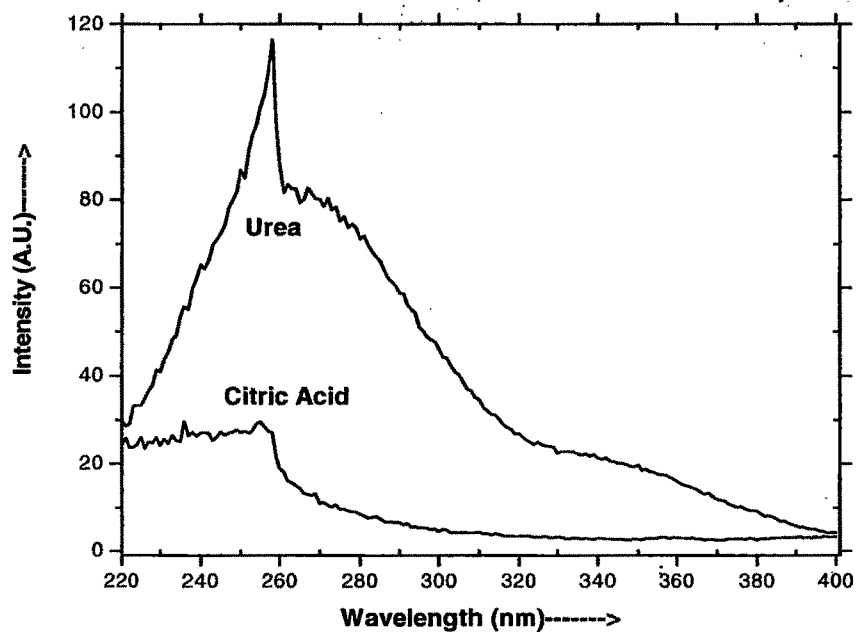


Figure-8 The photoluminescence excitation spectra of the combustion synthesized sample with different fuels monitored with 472nm wavelength.

The photoluminescence emission and excitation spectra of the combustion synthesized sample have been shown in figure-7 & 8 respectively with two different fuels (citric acid and Urea), the fuel are in Stoichiometry (neither fuel rich nor lean). The fuel used for the combustion synthesis was urea/citric acid, though there are many reports on the fuel used for combustion as carbohydrazide and ethylene glycol, but we have found that the carbohydrazide is very harmful for health (environmental hazard) as it produces carcinogenic gases during the reaction and ethylene glycol produces low flame temperature than the fuels that we have used [40]. Till date there is only one report on the synthesis of Sr_2CeO_4 by combustion [14] and they have used glycine/citric acid as the fuel but even they have not elaborated nor tried to study the effect of F/M ratio on the optical properties of the phosphor. Moreover we have used urea as the fuel to study the effect of F/M ratio and this is the first time that this fuel and such study (F/M ratio) on the nature of luminescence is done. The F/M ratio was also varied in some of the reactions to see the effect on the optical properties and the formation of the compounds. The F/M ratio is a very important parameter to get for getting good nanosize particles, fuel rich, fuel deficient and fuel equal variations were tried. The variation of the F/M ratio is given in table-3 for urea used as fuel. The luminescent measurements were carried out in identical conditions. Along with the study of the F/M ratio we have also studied the effect of further annealing of the phosphor at 1200°C. As in many cases of the combustion synthesized phosphors it is mentioned that for combustion synthesis further heat treatment is not required. Hence to find out the effect of heating on the photoluminescence characteristics we gave further heat treatment to the synthesized phosphors after the combustion at respective F/M ratios. The heat treatment of 1200°C for 3hrs is given to a part-whereas the second part is used as it is for further investigations.

Sample name (1200°C)	Sample name (as prepared)	Ratio F/M	Fuel
U-1	U-5	1.67:1	Urea
U-2	U-6	2.167:1	Urea
U-3	U-7	2.9:1	Urea
U-4	U-8	2.271:1	Urea

Table-3 Different F/M ratio along with the sample name.

Figure-7 & 8 shows the emission and excitation curves of the Sr_2CeO_4 combustion synthesis at 254nm and 469nm respectively. It is found that the intensity of the CA prepared fuel is very low in comparison to the Urea, this may be due to the fact that the adiabatic flame temperature when the combustion takes place are not high enough for the reaction to fully take place when the CA is used as fuel. This hinders the reaction mechanism and hence the lesser luminescence intensity, the product may also be with traces of the unreacted starting material. It was then imperative that the fuel used in the combustion reaction for further study was to be taken as urea and an elaborate understanding of the F/M ratio affecting the luminescence intensity and hence the resulting product. As urea is cheap and readily available commercially and generates the highest temperature, although fuel-rich mixtures might produce prematurely sintered particle agglomerates. Moreover, the combustion of hydrazide yields carcinogenic gases which are injurious to health and environment [28]. To investigate the influence of the ratio F/O in the redox mixture, mainly, to find out if urea contents below stoichiometry were enough to trigger the explosive combustion of the fuel and the subsequent decomposition of the salts.

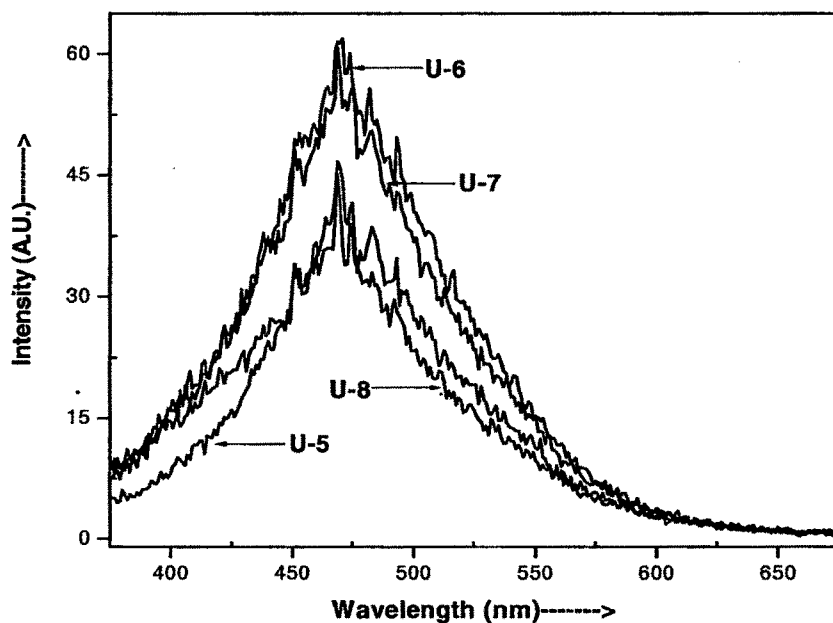


Figure-9 The photoluminescence emission spectra of the combustion synthesized sample with different F/M ratio at 254nm excitation wavelength.

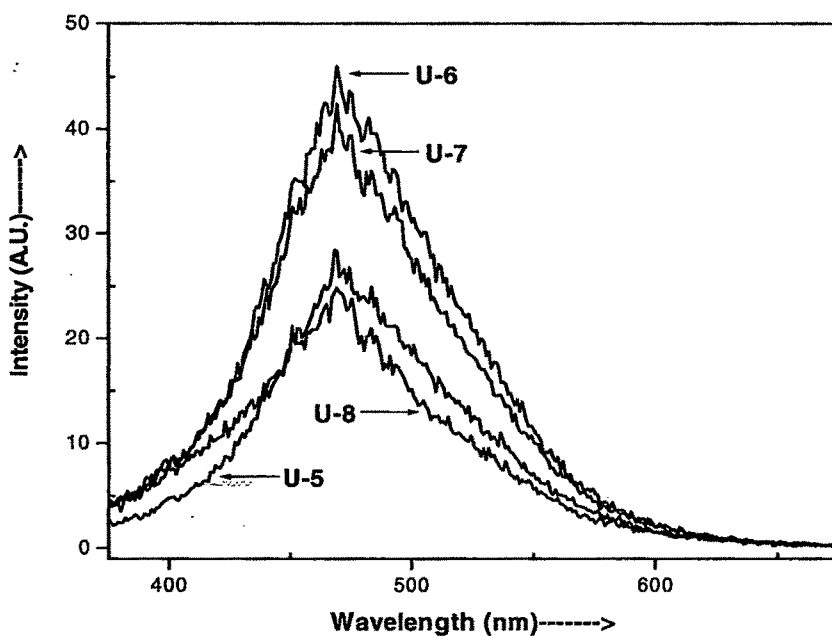


Figure-10 The photoluminescence emission spectra of the combustion synthesized sample with different F/M ratio at 280nm excitation wavelength.

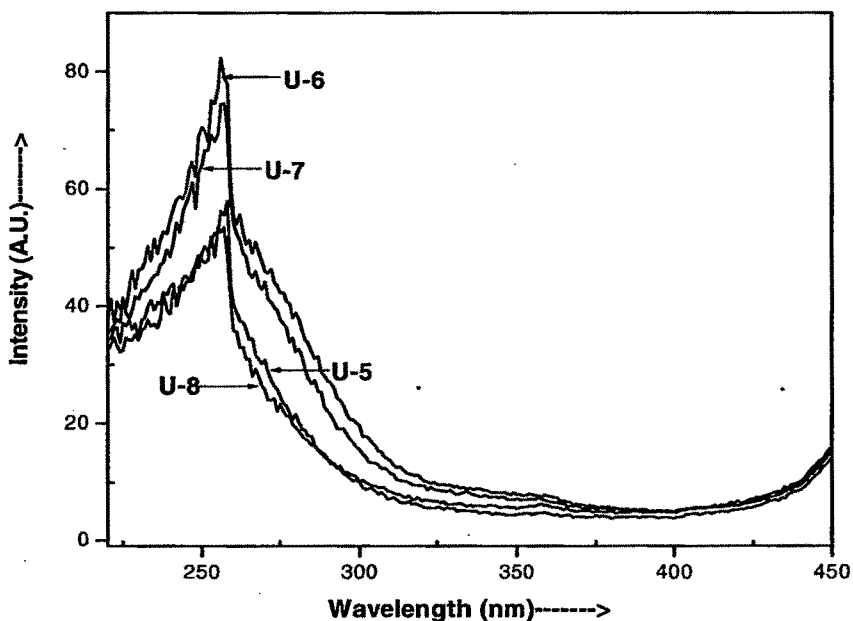


Figure-11 The photoluminescence excitation spectra of the combustion synthesized sample with different fuels at 254nm excitation wavelength.

The figure-9 & figure-10 shows the emission of combustion synthesized Sr_2CeO_4 (as prepared, without further heat treatment) sample for different F/M ratios when excited with 254nm and 280nm respectively. The interesting feature of this graph is that the sample shows negligible and very weak peaks and intensity at ~469nm, this confirms our prior conclusion that further heating is required for the combustion synthesized samples and the samples should be heated for the pure phase formation and moreover the intensity of the heat treated samples is high due to the high crystallinity of the product formed. The samples were monitored both at high and low sensitivity in the PL measurements and it was found that there is a difference only in the intensity, with peak positions appearing at the same place. The ratio between the high and low sensitivity is 50:1 and the same is observed in the intensity pattern of the curves.

The figure-11 is the excitation spectra of the phosphor when the monitored wavelength was kept at 469nm, the only difference lies in the peak intensity when the fuel deficient ratio was taken the intensity was lowest and for the fuel rich it was highest (2.16:1) but decreased as it was further increased. This may be due the fact that as the fuel ratio is near to the stoichiometry value (1.944:1 for the present case), the particle size is small and a high optical efficiency might be obtained, whereas, on addition of the fuel above a threshold value, the fluorescence light is probably extinguished by the NO_3^- in the resulting ash which tends to absorb H_2O from the environmental atmosphere [54]. Another assumption is also made, that the specimens prepared are usually in porous fuzzy form, so that H_2O , CO_2 and NO_2 molecules can persist in the sample even after the combustion is over. The last fact would be elucidated by checking the photoluminescence measurements after giving them further heat treatment.

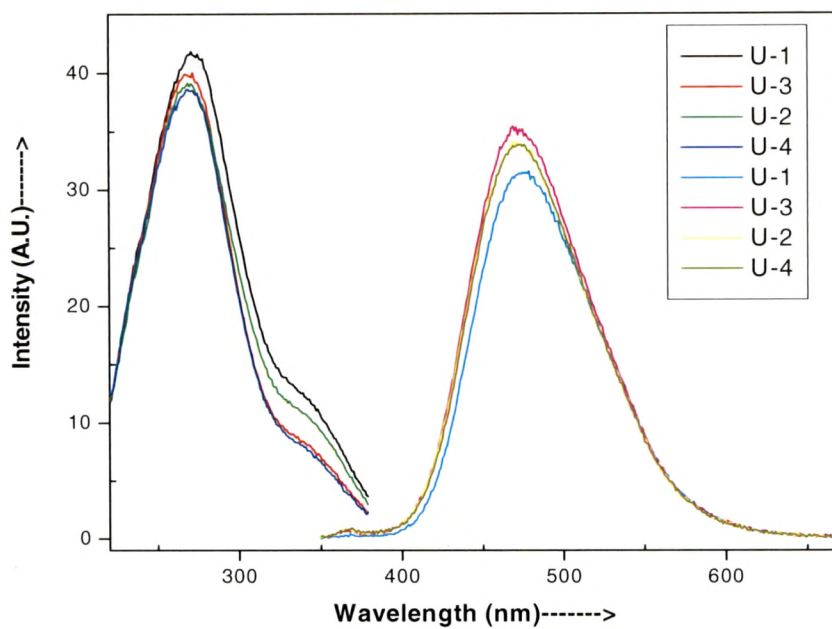


Figure-12 The photoluminescence emission and excitation spectra of the combustion synthesized sample with different F/M ratio monitored at 254nm and 469nm excitation wavelength.

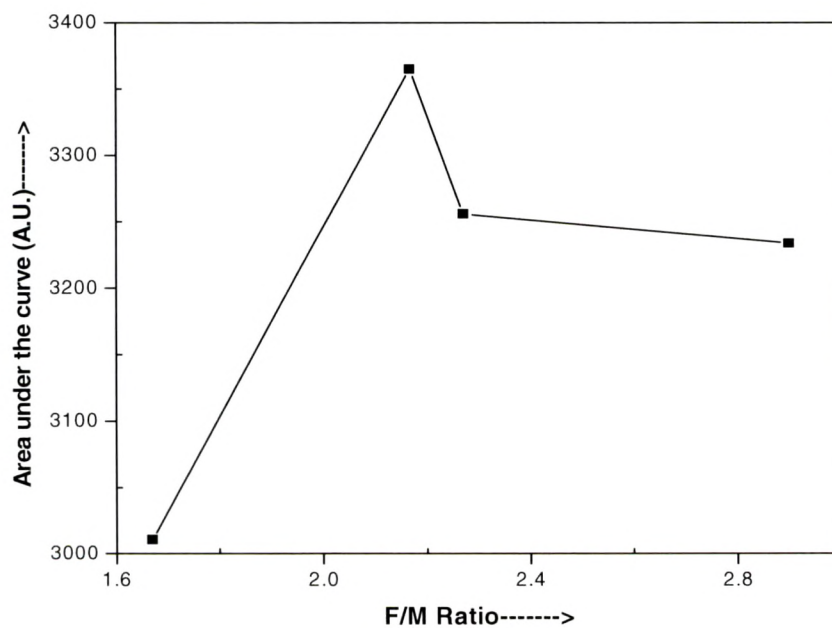


Figure-13 The variation of F/M ratio with area under the curve.

The figure-12 shows the emission and excitation of the combustion prepared sample with 254nm and 469nm respectively (heat treated further at 1200°C for 3hrs and PL monitored at low sensitivity), with different F/M ratio. The interesting observation that can be observed is that, despite the intensity being very low, the emission and excitation follows the same pattern. The F/M ratio has an increment or decrement effect on the intensity, the most important and remarkable effect is seen on the peak position of the emission curves. As the F/M ratio changes it has a remarkable effect on the position of emission, the fuel rich ratio (2.167 and 2.27) has the peak appearing at 469nm but with fuel excess sample (with F/M ratio as 2.9:1), the position of the maxima is at 479nm and for the fuel deficient sample (with F/M ratio as 1.67:1), the peak maxima is at 476nm. This remarkable 'blue shift' of around 10nm in the emission is due to the small size of the particle. The same was also evident with the sol-gel synthesized 800°C heated sample. Here it is imperative to mention that the different synthesis technique have resulted in peak position of the emission at different places, but in our case when the synthesis technique was either sol-gel or combustion the peak wavelength for the emission was 469nm, there is a shift of ~10nm towards the higher wavelength region. This may be attributed to the nanocrystallite size of the compound. The same is evident for the excitation curve, the shift in the peak from 269nm (for the 2.167:1 and 2.27:1 fuel rich ratio) to 271nm (for the 1.67:1 fuel lean ratio) and again to 272nm (for the highest F/M ratio (2.9:1)). This result elucidates the fact that it is not necessarily that fuel rich will get the desired property but there should be a judicious selection for the ratio and the fuel rich samples lead to good results. The fuel to oxidizer ratio has an effective role to play in the changing the size and thus the optical property of the phosphor. Figure-5 is the area under the each curve versus different F/M ratio. This clearly shows that the area under the curve increased as we increase from fuel deficient to fuel rich ratio but again decreases for a very high F/M ratio, this is in accordance with results obtained by others such as Chen et al [40], Bacalski et al [53] and Phan et al [54, 55].

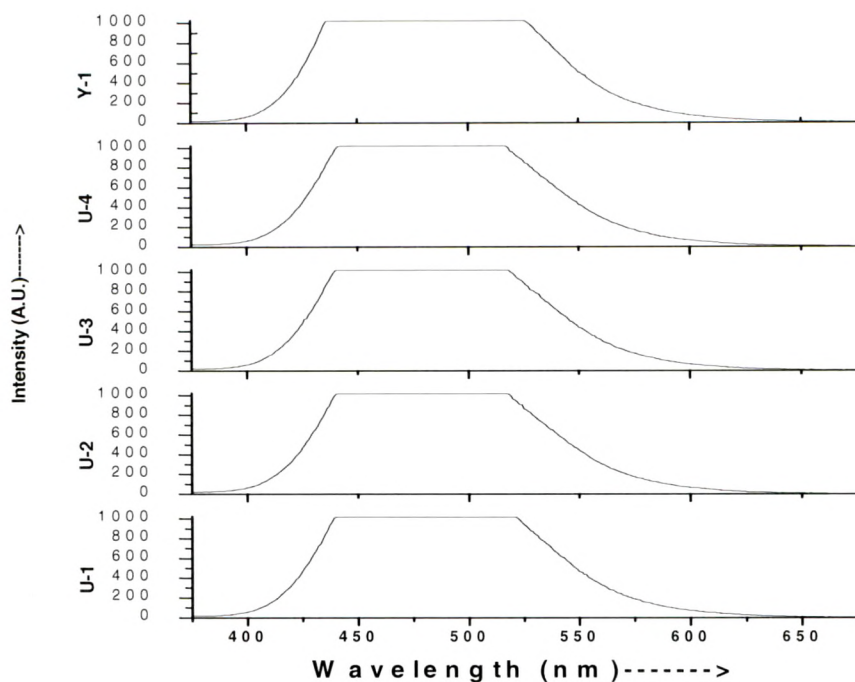


Figure-14 The photoluminescence emission spectra of the combustion synthesized sample with different F/M ratio excited at 254nm wavelength.

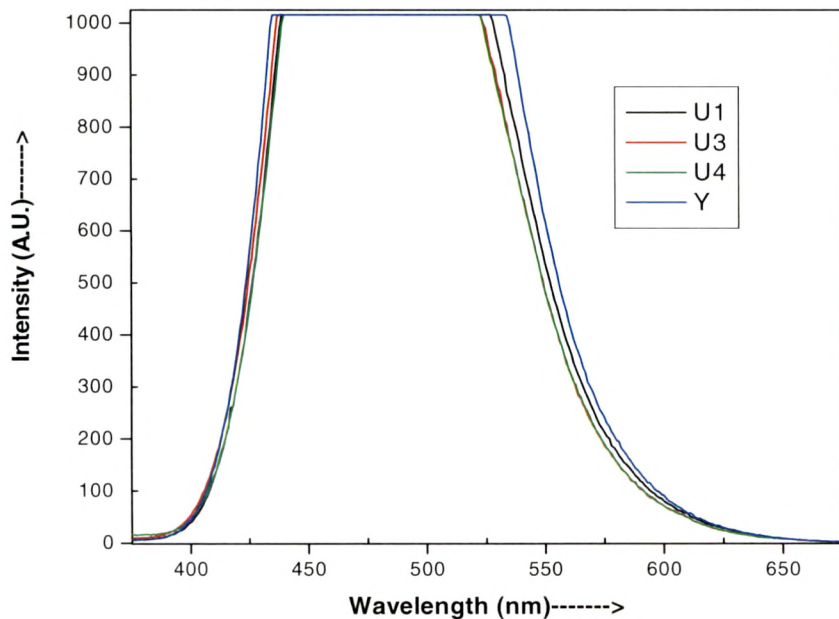


Figure-15 The photoluminescence emission spectra of the combustion synthesized sample with different F/M ratio excited at 280nm wavelength.

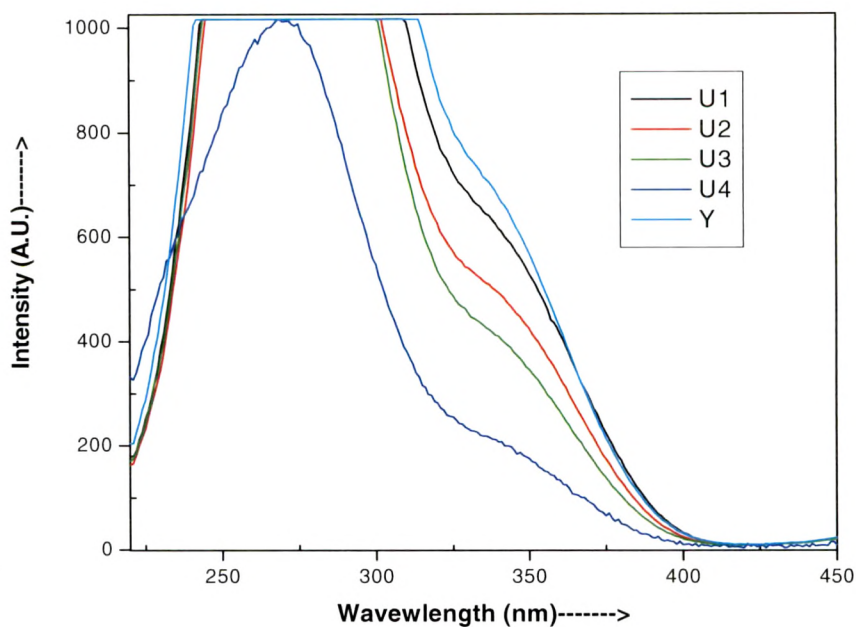


Figure-16 The photoluminescence excitation spectra of the combustion synthesized sample with different F/M ratio monitored with 471nm wavelength.

The figure-14 & 15 shows the emission spectra of the Sr_2CeO_4 sample (heat treated at 1200°C for 3hrs) with different fuel to metal ratio (shown in table-3) at different excitation with 254nm and 280nm respectively (at high sensitivity)(the samples marked Y in the figure is for sol-gel). These all synthesized samples are either fuel rich or fuel deficient as this is an important parameter in getting the right size with better optical properties. The increase of temperature affects the crystallinity as we see the sample intensity is out of range for the high sensitivity in the photoluminescence measurements. For comparison we have included a sol-gel (1200°C) sample, all the curves are out of range with the width and intensity of sample being maximum for the sol-gel sample followed by all others. The peak shape and the position do not seem to change with the change in either the F/M or even with the synthesis technique. For the measurements at low sensitivity this effect was more pronounced and it showed a variation in the peak position, we assume the shift to be there but it was not seen due to the intensity being out of range. The sol-gel prepared still has the highest intensity and the width of the sample is also maximum among all the prepared samples. The

positive feature of the sample prepared with the sol-gel is again highlighted with this result. The figure-16 shows the corresponding excitation curve of the sample when monitored with 471nm for the same conditions as defined for figure-14 & 15. The curves for combustion as well as for sol-gel synthesized sample are shown. Again the peak width and the intensity (out of range) for the sol-gel synthesized sample is highest followed with different F/M ratio sample. The interesting observation from the excitation curves is that the peak for all the samples is at ~254nm by a hump at the 270-280nm which again justifies the difference due to the two different bond lengths of the Ce-O in the Sr₂CeO₄ which has a difference of 0.1Å [67].

The transitions appearing are all due to the charge transfer transitions due to the fact that the Cerium in tetravalent state has empty f orbital and the oxygen act as ligand attached, thus the CTT takes place resulting from the Ce⁴⁺-O²⁻. The CTT transition is very rare and infact has been reported for the first time for Ce⁴⁺ in Sr₂CeO₄ phosphor, its early history dates back to Nakazawa who was the one to report the CTT for the first time in 1978 for Yb³⁺[71, 72] and also by Pieterse et al [73]. The appearance of the emission coming from the Ce⁴⁺ and not relating to the Ce³⁺ was to be checked though the phosphor had emission characteristics different to that coming from the Ce³⁺.

The appearance of two bands in the excitation spectra of the Sr₂CeO₄ was also surprising but later the reason for it was concluded that it was due to the different bond lengths of the Cerium attached with the oxygen ligand, one equatorial and the other terminal with the difference between them being ~ 0.01nm (0.1Å). Thus the excitation has two different excitation wavelengths. The appearance of the same in the excitation is unequivocally due to the reasons above. All the above synthesis technique and the results of photoluminescence have shown the maxima of the peak appears in between the 469-480nm (2.64-2.58eV). The absorption also originates from a charge transfer from O²⁻ to Ce⁴⁺, that is, the O 2p⁶→Ce 4f⁰ electronic transition (vide infra) [60]. This is also analogous with the results from the excitation spectra. The full width at half maxima (FWHM) for the emission band at 472nm is around 3900 cm⁻¹ for the sample prepared with combustion technique and it increases to ~5400 cm⁻¹ for the sample with intensity out of range for the samples prepared with sol-gel technique. These values were also reported by Nag et al [17] and Pieterse et al [59]. Stokes shift was also

estimated from the emission and excitation curves, it was found to be $\sim 8300\text{cm}^{-1}$. From the literature it is well established that the Stokes shift for a CT transition on a rare earth ion ranges between 4000cm^{-1} up to 17000cm^{-1} and the FWHM for the CT emission is typically between $3000\text{-}6000\text{cm}^{-1}$ [73]. For the present case of Sr_2CeO_4 the measured Stokes shift and FWHM fits in the range described. It is also well known that the CTT are sensitive to the ligand environment i.e. the potential field of the ligands [17]. No overlap was also found between the excitation and emission spectra. Except for the change in the intensity, no appreciable change was found when the sample was excited with wavelengths from 240-360nm. Similarly there was no difference in the spectra when it was monitored with 460-480nm except for the change in the intensity.

3.5.4 Thermoluminescence Studies

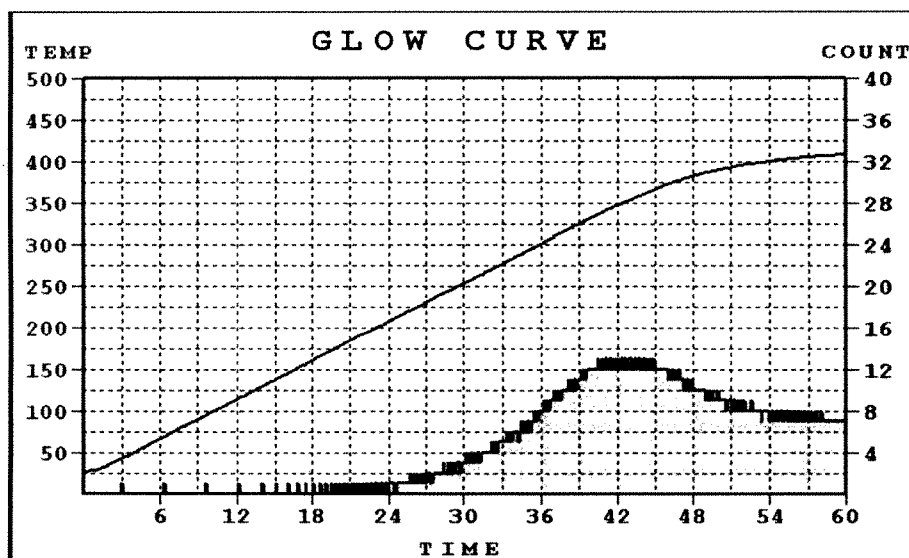


Figure-17 Thermoluminescence glow curve of Solid state Synthesized Sr_2CeO_4 .

The figure-17 shows the TL glow curve of the solid state synthesized Sr_2CeO_4 phosphor. The irradiation source used for the present study was Cobalt-60 (gamma) source, at a heating rate of $6.67^\circ\text{C}/\text{sec}$. it was found that there is no thermoluminescence glow curve peaked at around $\sim 340^\circ\text{C}$, this is very high. This can be attributed to the onset of the kanthal strip of the glow curve recorder. The sample was prepared by the solid state reaction technique. The sample was

irradiated with gamma rays of dose 1K Gy. The sample of sol-gel as well as combustion synthesized sample does not show any TL glow peak.

As the glow peak is observed at around $\sim 340^{\circ}\text{C}$ it is difficult to distinguish it with the background or the black body radiation of the kanthal strip. The black body radiation occurs generally from the kanthal strip at the higher temperature i.e., above 300°C . But the glow curve represented here is already deducted from the background counts.

The TL glow curve of the sol-gel as well as combustion synthesized samples shows the glow peak at around similar temperature but the left out after background deduction is too less to mention. The glow curve was measured for different gamma dose but at lower dose the curve was not clear and hence we have to exposed it with high doses.

The formation of the TL is represented in the following picture:

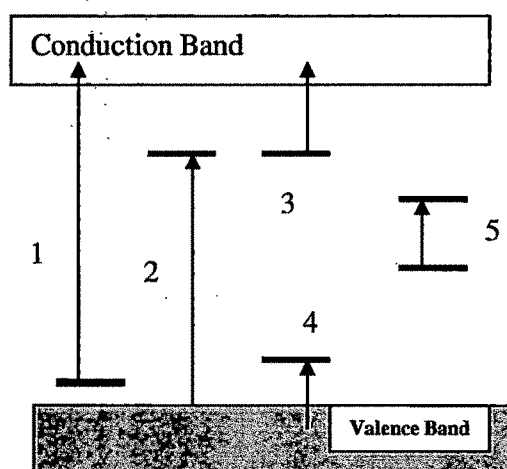


Figure-18 Schematic representation of the possible transitions in the insulator 1 & 2. Defect Ionization 3 & 4. Trap Ionization 5. Internal Intra-center Transition.

The figure-18 shows the different types of the transitions in the insulators. Where the transitions 1 & 2, 3 & 4 are responsible for the Thermoluminescence glow peak formation. In any material the formation of the TL glow peaks is depend on

the presence of the defects that create traps and recombination center in the host lattice. Generally, these defects are formed by addition of the dopant in the matrix or it may be formed due to the presence of impurities and different phases. In case of the solid state reaction synthesized sample the presence of impurities, unreacted raw material and the presence of other phases are already confirmed by the XRD studies. So it is obvious that this phosphor exhibits the TL glow curve. Whereas the sol-gel and combustion synthesized sample shows generally a single phase compound and also a minimum amount of impurity. This may be the reason behind the absence of the defects which gives TL in the phosphor.

The transition 5 depicted in the figure-18 shows the transition responsible for the PL emission and absorption. The luminescence emitted from the following absorption of light by an internal transition as shown in 5. Since this does not involve transport of charge from one defect site to another such transitions do not affect the TL signal.

3.5.5 Calculation of CIE coordinates for different method of synthesis

The Commission Internationale de l'Eclairage (CIE) coordinates were calculated using the Equidistant-wavelength method as described in the chapter-2. The different CIE coordinates reported till date for the Sr_2CeO_4 with different synthesis technique have been tabulated in table-4. The calculated CIE coordinates from the photoluminescence emission spectra have all been plotted in the diagram below and have also been tabulated in table-5 and 6. The table shows the sample name and the temperature at which the sample was synthesized. The samples have all been tabulated for better understanding. The table-4 has values that have been reported for the Sr_2CeO_4 by various workers till date, the interesting thing to be noticed here is that despite the different synthesis technique for all the compounds the coordinates are almost similar with the exception being of the Serra et al [12].

Sr. No.	CIE – X	CIE – Y	Reference
1.	0.198	0.292	Danielson et al [5]
2.	0.19	0.26	Jiang et al [8]
3.	0.16	0.21	Serra et al [12]
4.	0.20	0.28	Hirai et al [18]
5.	0.176	0.283	Xing Desong [22]
6.	0.20	0.27	Kang et al [64]

Table-4 The CIE coordinates reported in the literature for the Sr_2CeO_4 phosphor.

The already reported values, when compared with that of those prepared by the different synthesis technique show the variation with some of the reported values but are in good agreement with those of the Serra et al. The CIE coordinates for the sample prepared via solid state reaction, sol-gel and combustion reaction have been tabulated in table-5 and 6. The CIE coordinates for the samples have been calculated for CIE 1931, CIE 1960 and CIE 1976. Though the most common among them is the CIE 1931 but it suffers from drawbacks that are less with the CIE 1976, also known as uniform chromaticity scale diagram or the CIE 1976 UCS diagram commonly referred to as the u' , v' diagram.

The calculation of u , v , u' and v' have been done according to the given equations:

$$u = \frac{4x}{-2x+12y+3}, \quad v = \frac{6y}{-2x+12y+3} \quad \text{-----1}$$

$$u' = \frac{4x}{-2x+12y+3}, \quad v' = \frac{9x}{-2x+12y+3} \quad \text{-----2}$$

The u' , v' diagram is useful for showing the relationships between colours whenever the interest lies in their discriminability.

CIE co-ordinates	CIE 1931	CIE 1960	CIE 1976			
Sample Name	x	y	u	v	u'	v'
SG-800°C	0.167	0.247	0.119	0.263	0.119	0.395
SG-1000°C	0.160	0.254	0.112	0.266	0.112	0.399
SG-1200°C	0.162	0.258	0.112	0.268	0.112	0.402
SSR-1200°C(LS)	0.167	0.293	0.108	0.284	0.108	0.427
SSR-1200°C	0.175	0.302	0.112	0.289	0.112	0.433

Table-5 The CIE coordinates for the sol-gel and solid state synthesized Sr_2CeO_4 at different temperatures and different parameters (LS-Low Sensitivity).

The table-5 depicts the values of the CIE coordinates calculated for sol-gel and solid state synthesized samples at different temperatures and with different parameters (Low sensitivity in the PL set-up). There is no remarkable difference between those synthesized at 800°C, 1000°C and 1200°C for the sol-gel, all values are near to $x = 0.16$ and $y = 0.25$ matching with those of Serra et al [12] but do not match with the others as shown in table-4. Whereas for the solid state synthesis the values comes out to be around $x = 0.17$ and $y = 0.30$, with slight variation emission was monitored with low sensitivity in the PL measurements.

CIE Co-ordinates	CIE 1931		CIE 1960		CIE 1976	
	x	y	u	v	u'	v'
Sample Name						
U1-254nm	0.170	0.277	0.113	0.277	0.113	0.416
U2-254nm	0.167	0.270	0.113	0.274	0.113	0.411
U3-254nm	0.167	0.270	0.113	0.274	0.113	0.411
U4-254nm	0.166	0.269	0.113	0.274	0.113	0.411
U1-280nm	0.175	0.289	0.114	0.283	0.114	0.425
U2-280nm	0.170	0.304	0.111	0.290	0.111	0.434
U3-280nm	0.172	0.282	0.113	0.280	0.113	0.420
U4-280nm	0.170	0.281	0.113	0.279	0.113	0.419
Y1-254nm	0.162	0.258	0.112	0.268	0.112	0.402
Y2-250nm	0.169	0.275	0.113	0.277	0.113	0.415
Y3-240nm	0.156	0.233	0.113	0.255	0.113	0.382
Y4-280nm	0.179	0.295	0.116	0.286	0.116	0.429
Y5-310nm	0.159	0.251	0.111	0.264	0.111	0.397
Y6-340nm	0.156	0.240	0.112	0.258	0.112	0.388
Y7-360nm	0.157	0.236	0.113	0.256	0.113	0.385

Table-6 The calculated CIE coordinate values for the Combustion and Sol-Gel synthesized Sr_2CeO_4 at different conditions (Different excitations and F/M ratio) (Y is for sol-gel and U is combustion synthesized).

The calculated values for the CIE have been presented in table-6 are for combustion with different F/M ratio and for sol-gel at different excitation wavelengths. For the different F/M ratio there is hardly any difference in CIE coordinates appearing for the first 4 rows of the table-6. When excitation was kept at 280nm there was appreciable change in the CIE coordinates. The change is apparent and the coordinates shifted from $x = 0.16$, $y = 0.27$ to $x = 0.17$, $y = 0.28$.

Similarly the CIE coordinates were evaluated for the sol-gel synthesized samples for different excitation wavelengths from 240-360nm and are tabulated in table-6. It was observed that the CIE coordinates are almost similar when the excitation was kept at 240, 310, 340 and 360nm respectively. When the excitation was kept at 250, 254 and 280nm the values were found to be very similar and better when

compared to the solid state and the combustion synthesized ones. This is another positive feature of the sample synthesized using the sol-gel technique, getting good color coordinates, this in turn leads to better chromaticity, hence improving the overall color rendering index of the phosphors.

3.6 Conclusions

The main conclusions that can be drawn from these are as follows:

1. Powder samples of Sr_2CeO_4 prepared by the sol-gel technique exhibits high homogeneity, more uniformity and uniform nano crystalline size (~45nm) as compared to the sample prepared by solid state reaction process (~155nm).
2. Control over the size and the results appearing in the nano regime are instrumental in applying the sol-gel for the production of nanocrystal with better optical properties.
3. The luminescence intensity is also higher in the former case; further, the photoluminescence intensity increases as the firing temperature was increased from 800 to 1200°C.
4. The duration of firing was also very less for the sol-gel prepared sample when compared to the one prepared by solid state reaction technique.
5. Morphology and the shape of the sol-gel is spheroidal which can enhance the luminescence intensity whereas on the other hand the solid state synthesized were heavily agglomerated which diminishes the luminescence intensity to an extent and are serious drawbacks for applications.
6. Sol-Gel synthesis has many positive features which makes them an exciting and useful synthesis tool for oxide synthesis.
7. The combustion synthesis was also tried and compared with the sol-gel synthesized, it was found that the sol-gel synthesis prepared one still has better luminescence characteristics.
8. For the combustion synthesis fuel to oxidizer ratio is also an important parameter and the variation of the same was done to check the effect on the luminescent characteristics of the synthesized phosphor. It was found that a F/M ratio directly effect the luminescent properties and fuel lean and fuel rich sample had less intensity.

9. Judicious use and application for making the phosphor with better luminescent properties the F/M ratio should be fuel rich rather than the fuel deficient.
10. There was remarkable 'blue shift' in the emission and excitation spectra for the sol-gel synthesized and the combustion. This may be due to the formation of uniform nanosize particles showing blue shift in the luminescence emission from Sr_2CeO_4 .
11. CIE coordinates evaluated also suggest that the sol-gel prepared sample had the better chromaticity values compared with the solid state and the combustion synthesized.
12. The main limitations of the solid state synthesis are the inhomogeneous nature of the product.
13. Formation of particles with low surface area and hence mechanical particle size reduction required with grinders etc, which results in the introduction of impurity and defects.
14. Presence of defects quenches the luminescence.
15. Morphology by Scanning electron microscopy for the sol-gel synthesized also suggest better shape particles compared with those by solid state reaction which were found to be agglomerated at high temperatures and long duration of firing by the solid state reaction.
16. Experimental results show that this phosphor can be a suitable candidate for field emission displays as well as in fluorescent lamps because of the excitation being by UV~254nm which coincides with that of the Mercury (Hg) emission in the fluorescent lamps.
17. The solid state synthesis has properties that are detrimental in getting the right optical properties and hence sol-gel offers a new alternate for getting the desired optical property.

References

- [1] R.N. Bhargava, D. Gallagher, *Physical Review Letters*, 72, (1994), 416.
- [2] O.A. Graeve, S. Varma, G. Rojas-George, D.R. Brown, E.A. Lopez, *Journal of American Ceramic Society*, 89, (3), (2006), 926–931.
- [3] A.M. Chinie, A. Stefan, S. Georgescu, *Romanian Reports in Physics*, 57, 3, (2005), 412-417.
- [4] G. Wakefield, H.A. Keron, P.J. Dobson, J.L. Hutchison, *Journal of Colloid and Interface Science*, 215, (1999), 179-182.
- [5] E. Danielson, M. Devenney, D. Giaquinta, J.H. Golden, R.C. Haushalter, W. McFarland, D.M. Poojary, C.M. Reaves, W. Henry Weinberg, X.D. Wu, *Science* 279 (1998) 837.
- [6] *Luminescent Materials*, G. Blasse and B.C. Grabmaier, Springer Verlag, Berlin, (1994), Chapter-2, Page 11-19.
- [7] C.H. Park, C. Kim, C. Pyun, J. Choy, *Journal of Luminescence*, 87-89, (2000), 1062-1064.
- [8] Y.D. Jiang, F. Zhang, C.J. Summers, Z.L. Wang, *Applied Physics Letters*, 74, (12), (1999), 1677-1679.
- [9] Y. Tang, H. Guo, Q. Qin, *Solid State Communications*, 121, (6-7), (2002), 351-356.
- [10] M. Kang, S. Choi, *Journal of Material Science*, 37 (2002) 272.
- [11] Y.E. Lee, D.P. Norton, J.D. Budai, P.D. Rack, M.D. Potter, *Applied Physics Letters*, 77, (5), (2000), 678.
- [12] O.A. Serra, V.P. Severino, P.S. Calefi, S.A. Cicillini, *Journals of Alloys and Compounds*, 323-324, (2001), 667-669.
- [13] X. Yu, X.H. He, S. Yang, X. Yang, X. Xu, *Materials Letters*, 58, (2003), 48-50.
- [14] J. Gomes, A.M. Pires, O.A. Serra, *Quimica Nova*, 27, (2004), 5.
- [15] Y.B. Kholam, S.B. Deshpande, P.K. Khanna, P.A. Joy, H.S. Potdar, *Materials Letters*, 58, (20), (2004), 2521-2524.
- [16] S. Chen, X. Chen, Z. Yu, J. Hong, Z. Xue, X.Z. You, *Solid State Communications*, 130, (3-4), (2004), 48-50.
- [17] A. Nag, T.R.N. Kutty, *Journal of Materials Chemistry*, 13, (2003), 370-376.

- [18] T. Hirai, Y. Kawamura, *Journal of Physical Chemistry B*, 108, (2004), 12763-12769.
- [19] T. Hirai, Y. Kawamura, *Journal of Physical Chemistry B*, 109, (2005), 5569-5573.
- [20] H. Kim, Y.T. Kim, H.K. Chae, Y. Dong, H. Yun, *Journal of Sol-Gel Science and Technology*, 33, (2005), 75-80.
- [21] N. Perea, G.A. Hirata, *Optical Materials*, 27, (2005), 1212-1216.
- [22] D. Xing, J. Shi, M. Gong, *Materials letters*, 59, (2005), 948-952.
- [23] S. Shi, J. Li, J. Zhou, *Materials Science Forum*, 475-479, (2005), 1181-1184.
- [24] M.L. Pang, J. Lin, S.B. Wang, M. Yu, Y.H. Zhou, X.M. Han, *Journal Physics: Condensed Matter*, 15, (2003), 5157-5169.
- [25] K. Somaiah, H. Neelima, M. Vithal, K. Koteswara Rao, D.K. Avasthi, F. Singh, *Proc. Of NCLA*, (2003), New Delhi, P.96.
- [26] G. Wakefield, H.A. Keron, P.J. Dobson, J.L. Hutchison, *Journal of Colloid and Interface Science*, 215, (1999), 179-182.
- [27] G. Wakefield, H.A. Keron, P.J. Dobson, J.L. Hutchison, *Journal of Physics and Chemistry of Solids*, 60, (1999), 503-508.
- [28] S. Ekambaram, K.C. Patil, M. Maaza, *Journal of Alloys and Compounds*, 393, (2005), 81-92.
- [29] J.N. Hay, D. Porter, H.M. Raval, *J. Mater. Chem.*, 10, (2000), 1811-1818.
- [30] M. P. Pechini, (1967), *US Patent Specification*, 3, 330, 697.
- [31] A.M. Chinie, A. Stefan, S. Georgescu, *Romanian Reports in Physics*, 57, 3, (2005), 412-417.
- [32] N. Zhua, Y. Lia, X. Yua, W. Ge, *Journal of Luminescence*, 122-123, (2007), 704-706.
- [33] G. Frenzer, W.F. Maier, *Annual Reviews in Material Research*, 36, (2006), 281-331.
- [34] C. Tsai, H. Teng, *Journal of American Ceramic Society*, 87, (11), (2004), 2080-2085,
- [35] J. Zhang, Z. Zhang, Z. Tang, Y. Lin, *Journal of American Ceramic Society*, 85, (4), (2002), 998-1000.

- [36] D. Wang, Y. Li, Y. Xiong, Q. Yin, *Journal of The Electrochemical Society*, 152, (2005), H12-H14.
- [37] D. Dong, Y. Yang, B. Ziang, *Materials Chemistry and Physics*, 95, (2006), 89-93.
- [38] M. Alifanti, B. Baps, Blangenois, *Chem. Mater.*, 15, (2), (2003), 395.
- [39] R. Reisfield, T. Saraidarov, *Optical Materials*, 28, (2006), 64-70
- [40] W. Chen, F. Li, J. Yu, *Materials Letters*, 60, (2006), 57-62.
- [41] J.J. Kingsley, K.C. Patil, *Mater. Lett.*, 6, (1988), 427.
- [42] K.C. Patil, S.T. Aruna, S. Ekambaram, *Curr. Opin. Solid State Mater. Sci.*, 2, (1997), 158.
- [43] S.S. Manoharan, K.C. Patil, *Journal of American Ceramic Society*, 75, (4), (1992), 1012.
- [44] J.J. Kingsley, K. Suresh. K.C. Patil, *Journal Solid State chemistry*, 88, (1990), 435-442.
- [45] S. Ekambaram, K.C. Patil, *Bull. Mater. Sci.*, 18, (1995), 921.
- [46] S. Ekambaram, K.C. Patil, *J. Alloys Compd.*, 217, (1995), 104.
- [47] S. Ekambaram, K.C. Patil, *J. Mater. Chem.*, 5, (1995), 905.
- [48] S. Ekambaram, K.C. Patil, *J. Alloys Compd.*, 248, (1997), 7.
- [49] S. Ekambaram, K.C. Patil, *J. Mater. Synth. Process.*, 4, (1996), 337.
- [50] J.J. Kingsley. N. Manickam, K.C. Patil, *Bulletin of Material Science*, 13,(3), (1990), 179-189.
- [51] K. C. Patil, *Bulletin of Material Science*, 16, (6), (1993), 533-541.
- [52] D.A. Fumo, M.R. Morelli, A.M. Segadeas, *Materials Research Bulletin*, 13, (10), (1996), 1243-1255.
- [53] C.F. Bacalski, M.A. Cherry, G.A. Hirata, J.M. McKittrick, J. Mourant, *Journal of SID Supplement-I*, (2000), 93-98.
- [54] T. Phan, M. Phan, N. Vu, T.K. Anh, S. Yu, *Phys. Stat. Sol.(a)*, 201,(9), (2004), 2170-2174.
- [55] T. Phan, V. Phan, S. Yu, M. Phan, Y. Chung, *Journal of the Korean Physical Society*, 45, (3), (2004), 709-712.
- [56] M. Daldosso, J. Sokolnicki, L. Kepinski, J. Legendziewicz, A. Speghini, M. Bettinelli, *Journal of Luminescence*, 122-123, (2007), 858-861.

- [57] N. Vu, T.K. Anh, G. Yi, W. Streck, *Journal of Luminescence*, 122–123, (2007), 776-779.
- [58] J. Chang, S. Xiong, H. Peng, L. Sun, S. Lu, F. You, S. Huang, *Journal of Luminescence*, 122-123, (2007), 844-846.
- [59] L. van Pieterse, S. Sovarna, A. Meijerink, *Journal of The Electrochemical Society*, 147, (12), (2000), 4688-4691.
- [60] F. Goubin, X. Rocquefelte, M. Whangbo, Y. Montradi, R. Brec, S. Jobic, *Chem. Mater.*, 16, (2004), 662-669.
- [61] S.V. Chavan, A.K. Tyagi, *Thermochimica Acta*, 390, (2002), 79-82.
- [62] R. Sankar, G.V. Subba Rao, *Journal of The Electrochemical Society*, 147, (2000), 2773-2779.
- [63] T. Masui, T. Chiga, N. Imanaka, G. Adachi, *Materials Research Bulletin*, 38, (2003), 17-24.
- [64] M. Kang, S. Choi, *Journal of Materials Science*, 37, (2002), 2721-2729.
- [65] S.K. Hong, D.S. Jung, H.J. Lee, Y.C. Kang, *Korean Journal of Chemical Engineering*, 23, (2006), 496-498.
- [66] X. He, W. Li, Q. Zhou, *Materials Science and Engineering-B*, 134, (2006), 59-62.
- [67] E. Danielson, M. Devenney, D. Giaquinta, J.H. Golden, R.C. Haushalter, W. McFarland, D.M. Poojary, C.M. Reeves, W. Henry Weinberg, X.D. Wu, *Journal of Molecular Structure*, 470, (1998), 229-235.
- [68] R. Pankajavalli, K. Annanthasivan, S. Anthonysamy, P.R. Vasudeva Rao, *Journal of Nuclear Materials*, 336, (2005), 177-184.
- [69] JCPDS card No. 22-1422.
- [70] T. Gfroerer, *Encyclopedia of Analytical Chemistry*, Edited by R.A. Meyers, (2000), 9209-9231.
- [71] E. Nakazawa, *Chemical Physics Letters*, 56, (1978), 161.
- [72] E. Nakazawa, *Journal of Luminescence*, 18/19, (1979), 272.
- [73] L. van Pieterse, M. Heeroma, E. de Heer, and A. Meijerink, *Journal of Luminescence*, 91, (2000), 177.